PCMDI Report No. 38

Climatology of East Asian Winter Monsoon and Cold Surges: Results from the 1979-1995 NCEP/NCAR Reanalysis

Yi Zhang, Kenneth R. Sperber and James S. Boyle
Program for Climate Model Diagnosis and Intercomparison
Lawrence Livermore National Laboratory, Livermore, CA 94550

October 1996

Table of Contents

Abstract

This paper presents the climatology of the East Asian winter monsoon and cold surges based on the 1979-1995 NCEP/NCAR reanalysis. In addition to documenting the frequency, intensity, and preferred propagation tracks of cold surges and the evolution patterns of associated fields, the temporal distribution of the Siberian high and cold surges is discussed. Further, this study examines the interannual variation of the winter monsoon and cold surges and its relationship with ENSO.

There are on average thirteen cold surges in each winter season (October to April), of which two are strong cases. The averaged intensity of cold surges, measured by maximum surface pressure, is 1053 hPa. The cold surges originate from two primary source regions: 1) northwest of Lake Baikal, and 2) north of Lake Balkhash. The typical evolution of a cold surge occurs over the period of 5-14 days. Trajectory and correlation analyses indicate that, during this time high pressure centers propagate southeastward around the edge of the Tibetan Plateau from the mentioned source regions. Some of these high pressure centers then move eastward and diminish over the ocean, while others proceed southward. The signature of the associated temperature, wind, and pressure fields propagate farther southward and

eastward. The affected area encompasses the bulk of the maritime continent. Although the intensity of the Siberian high is found to peak during December and January, the frequency of cold surges has a maximum in November and in March. This result suggests that November through March should be considered as the East Asian winter monsoon season.

Two stratifications of cold surges are used to examine the relationship between ENSO and the interannual variation of the winter monsoon. The first one, described as the conventional cold surges, indicates that the cold surge frequency reaches a minimum a year after El Nino events. The second one, defined as the maximum wind events near the South China Sea, shares the same source regions as the first. This stratification of surges is found to be in good agreement with the Southern Oscillation Index (SOI). Low SOI (high SOI) events coincide with high (low) frequencies of cold surges.

The interannual variation of averaged meridional wind near the South China Sea and the maritime continent is dominated by the South China Sea cold surges, and is also well correlated (R=0.82) with the SOI. Strong wind seasons are associated with La Nina and high SOI events; likewise, weak wind years are linked with El Nino and low SOI cases. This pattern is restricted north of the equator within the region of (0°N-20°N, 110°E-130°E), and is confined to the near surface layer. The surface Siberian high, 500 hPa trough and 200 hPa jetstream, all representing the large-scale monsoon flow, are found to be weaker than normal during El Nino years. In particular, the interannual variation of the Siberian high is in general agreement with the SOI.

Return to Table of Contents

---

1. Introduction

The East Asian winter monsoon, which is associated with a strong Siberian high and active cold surges, is one of the most energetic monsoon circulation systems. The dramatic shift of the northeasterlies and the outbreak of cold surges dominate the winter weather and climate in the East Asian region. The winter monsoon and cold surges exert a strong impact on the extratropical and tropical planetary-scale circulations (Chang and Lau, 1982), and influence the SSTs in the tropical western Pacific (Chang et al., 1979). Their general characteristics and the possible linkage between cold surges and tropical atmospheric and oceanic phenomena have been examined in many studies. For example, Chang and Lau (1982) showed that the outbreak of winter monsoon surges forced short term changes in the Hadley and Walker Circulation, the East Asian jetstream and large-scale deep convection over the equatorial western Pacific. Boyle (1986a, 1986b) found that the frequency and intensity of the monsoon surges for a given month were related to the intensity of the East Asian jetstream and the extratropical large-scale circulation patterns. Lau and Chang (1987) suggested that the interannual variations of the winter monsoon and cold surges may be related to ENSO and tropical intraseasonal oscillations. Ding and Krishnamurti (1987) noted an eastward shift of the tropical planetary scale divergent circulation in association with the cold surges which was very similar to the shift of the divergent circulation between El Nino and La Nina years.

However, little attention has been given to the climatological aspects of the winter monsoon and cold surges. Boyle and Chang (1984) documented the mean winter circulation statistics based on the Navy Fleet Numerical Oceanography Center's (FNOC) gridded analyses. Pan et al. (1985) compiled the statistics of the Siberian high and cold air outbreaks in China with emphasis on the effect to local weather

forecast. Ding and Krishnamurti (1987) summarized the climatological tracks of cold surges based on the data from the winter (DJF) of 1980 to 1984. Although the winter monsoon was much weaker than normal during the 1982-83 El Nino event (Lau and Chang, 1987), there has never been a systematic investigation on the relationship between ENSO and the interannual variation of the winter monsoon and cold surges.

The purpose of this study is to present the climatology of cold surges and the Siberian high based on the 1979-1995 NCEP/NCAR reanalysis. We emphasize the temporal and spatial distribution of the cold surges and the Siberian high, their origin, propagation paths and evolution patterns. Of particular interest is the interannual variation of winter monsoon and cold surges. Given that the winter monsoon activity was weaker during the 1982-83 period, one of our goals is to determine if a consistent relationship exists between ENSO and the interannual variation of the winter monsoon and cold surges.

Return to Table of Contents

---

2. Description of the reanalysis

We use twice-daily surface and upper-air fields from the NCEP/NCAR reanalysis (Kalnay et al., 1996) for the period of 1979-1995. The surface quantities include temperature, wind, and sea-level-pressure (SLP); upper-air fields are winds at 925 hPa, 850 hPa, 700 hPa, and 200 hPa and geopotential height at 500 hPa. The advantage of this data set is that the reanalysis used a "frozen" state-of-the-art analysis/forecast system to perform the data assimilation throughout the whole period, thus circumventing problems with previous numerical weather prediction analyses due to changes in techniques, models and data assimilation. Also, this dynamically consistent reanalysis offers good horizontal (2.5° x 2.5°) and vertical resolution (17 levels).

3. Winter monsoon circulation

3.1 Mean state

The winter monsoon circulation has been documented by many authors (e.g., Boyle and Chang 1984; Lau and Li 1984; Lau and Chang 1987; Boyle and Chen 1987) and is summarized here to serve as a background for this paper. The dominant surface feature of the winter monsoon is the Siberian high. The winter SLP averaged from 1979/80 - 1994/95 is shown in Fig. 1. This surface pressure system, with central pressure in excess of 1036 hPa, covers the entire East Asian continent and yields northeasterly flow over a large part of Asia. At 500 hPa, the flow pattern is dominated by the coastal trough. The intensity of this trough is quasi-geostrophically linked to the surface Siberian high. At 200 hPa, the most prominent feature is the East Asian jet near Japan. This jet, the strongest on the globe, is associated with intense baroclinicity, large vertical wind shear and strong cold advection. It is maintained by the Coriolis torque acceleration exerted on the ageostrophic wind near the jet entrance region. Its strength is inherently related to the intensity of the surface Siberian high and the 500 hPa trough. These features characterize the three-dimensional large-scale monsoon circulation.

Fig. 1 also presented the winter (DJF) surface wind averaged from 1979/80 - 1994/95. This climatological surface wind represents contributions from both the quasi-stationary Siberian high and the cold surges. North of 30°N, the wind blows along the north and east periphery of the Siberian high. This anticyclonic flow pattern is a reflection of the quasi-stationary pressure system. South of 30°N where the Siberian high pressure exerts less influence, the wind maximum near the South China Sea can be largely

attributed to the cumulative effects of the cold surges. One of the main features of this field is that the westerly flow near Japan bifurcates. The eastward branch merges with the Aleutian low; the southern branch joins the tradewind belt. Cold air intensity and thickness usually reduce significantly as the airmass moves southward. Thus, the winter monsoon is a shallow phenomenon in lower latitudes.

Return to Table of Contents

3.2 Variance of SLP and surface air temperature

The standard deviation of SLP in Fig. 2 (a) indicates that the Siberian high pressure is a rather stationary feature of the winter monsoon. The largest variations occur to the northwest of the Siberian high, and to the east where the variability near the Aleutian low dominates. Although the standard deviation of temperature is largest at high latitudes as indicated in Fig. 2 (b), substantial variability also occurs over eastern China. This is noticed as a pronounced southward extension of the standard deviation over this region. A similar, but less well defined southward extension is also seen in the variability of SLP. The southward extensions in both variables is an indication of the cold surge activity.

Figs. 2 (c) and (d) show the percent of total variance of SLP and surface air temperature explained by periods of 6-14 days, the typical lifetime of cold surges. Along the east coast of China, over 25% of the total variance of surface air temperature and SLP occurs on time scales of 6-14 days. The structure of the temperature variation exhibits more regionality than that of SLP and has a pronounced signal over eastern China. Power spectra of the surface air temperature and SLP in this vicinity exhibits many common spectral peaks on these time scales (not shown) suggesting a close association between the temperature and SLP variation in this region, which is consistent with the characteristics of cold surges. The substantial SLP variance over the Pacific Ocean near 25°N and the one northward over Japan are not necessarily associated with cold surge activity. These variation maxima are intriguing features of the SLP which will be investigated in future works. Cold air activity over the East Asia continent and the South China Sea will be of interest here.

4. Cold surges and Siberian high

The cold surges are the most important transient disturbances embedded within the mean monsoon circulation. The occurrence of a cold surge is characterized by a southward movement of a surface anticyclone and an associated abrupt 24-48 hours surface air temperature drop in the affected regions. The typical scenario of a cold air outbreak is: the Siberian high and the coastal trough reach a certain intensity. Further west over the continent, an upper level short wave undergoes strong development as it moves eastward. Eventually, the short wave develops into a major trough and replaces the old quasi-stationary coastal trough. During this process, a surface anticyclone moves southward and a cold surge occurs (Staff members of Academia Sinica, 1957). It should be pointed out that the build-up and maintenance of the Siberian high pressure is a necessary condition for the occurrence of cold surges. Radiative cooling, persistent cold air advection (usually blocking over Urals) throughout the troposphere and large-scale descending motion all contribute to the maintenance of the cold Siberian high (Ding and Krishnamurti,1987). However, cold surges should not be regarded as the simple southward expansion or temporal variability of the Siberian highs. Rather, it is of a separate dynamical entity. The Siberian high and the cold surge are the two most characteristic weather phenomena of the winter monsoon. The relationship between the two will be further discussed in Section 4.2.

Return to Table of Contents

4.1 Criteria for cold surges

Objective criteria to identify the cold surges are required in this study. Many cold surge definitions can be found in the literature. A summary of the often used definitions is given in Boyle and Chen (1987). Some of the cold surges are purposely defined for the convenience of weather forecasting. Definitions vary depending on regions of interest. For example, cold surges defined over the South China Sea may have nothing to do with cold surges defined near Korea. The essence of the cold surges, as mentioned above, is the rapid south-southeastward movement of a surface anticyclone, which brings significant surface air temperature drop in the affected regions.

In defining a cold surge from the reanalysis, we choose to average the necessary fields at particular regions which encompass a nine-grid-point rectangular at the 2.5° x 2.5° resolution (see Fig. 3). Region 1 is in southern Siberia, region 2 is in the middle of China, and region 3 covers part of southern China. Using information from these regions, we define a cold surge as follows:

1) Outbreak requires, (a) a surface anticyclone must be identified (Criteria in Zhang and Wang, 1996) in the vicinity of region 1, which has an averaged SLP >1035 hPa, and (b) During the movement of a surface anticyclone, the 24-48 hour surface air tem-perature drop must exceed 9°C in region 2, or 6°C in region 3.

2) Ending of a cold surge occurs when, (a) a negative pressure tendency at the anticy-clone center has persisted for 24 hours and the center pressure is <1025 hPa, and (b) positive surface temperature trend was found over 50% of the grid points in the bulk of the East Asia continent (102.5°E-117.5°E, 25°N-50°N).

A cold surge is chosen when these criteria are met. The thresholds, mostly based on synoptic experience, can be altered within a certain range. Despite this, the overwhelming majority of surges will still be identified because the key characteristics of cold surges are represented by these criteria. Also, since a cold surge affects large areas of East Asia in temperature and pressure fields, it is unlikely that a non-surge event will be identified as a surge.

In order to verify the identified cold surges, time series of surface air temperature in regions 1, 2, and 3 (T1, T2, and T3) of the 1987/88 winter are plotted in Fig. 4. According to the criteria, if a surface anticyclone has reached a certain intensity, a required drop in either T2 or T3 will qualify the disturbance to be a cold surge. All the observed cold surges during this season-known from other sources-were found to be associated with a temperature drop in region 2 or region 3. Fig. 4 illustrates how quickly the temperature can drop in a specific location and its southward propagation. One of the strongest cold surges ever observed occurred during late November of 1987. The recorded maximum surface pressure is in excess of 1081 hPa; the temperature drops are ~ 15°C in all three regions.

The timing, duration, and frequency of cold surges identified using this criteria are further compared with those defined operationally by the Beijing Meteorological Center (BMC) for the period 1979-84 (the period for which the data from BMC are available) and good agreement were found between the two. Thus, we have confidence that the cold surge definition is appropriate given the verification provided from in situ observations.

Return to Table of Contents

4.2 Statistics, trajectories and spatial evolution of cold surges

Based on the above criteria, over 200 cold surges have been identified during the 1979-95 period. Table 1 gives the average frequency, intensity, and duration for cold surges and strong cold surges. Strong cases are defined as events that are associated with temperature drop >10°C and northerly wind > 4 m s-1 in region 3. By the addition of this wind criterion, the strong cases are assured to be cold surges that exert impacts in the tropical region. The average maximum center pressure is ~1060 hPa for strong surges, and it is ~ 1053 hPa for all cold surges. Lifetimes of individual surges range from 5 - 14 days, with an average duration of ~7 days for cold surges and ~ 9 days for strong events.

Table 1: Cold surge statistics based on 16 winter seasons (1979/80-1994/950

	Number of Events/year	SLP intensity	Duration
All surges	13	1053 hPa	7 days
Strong surges	2	1060 hPa	9 days

The trajectories of the surface anticyclones associated with each of the cold surges are shown in Fig. 5. The circles indicate the original location of the high pressure center and the squares denote the termination points. Based on the trajectories, cold surges tend to originate from two distinct regions. The first is located northwest of Lake Baikal near 95°E-105°E, 45°N-60°N, and the second is to the north of Lake Balkhash and near 75°E-90°E, 52°N-60°N. All the surges propagate southward or southeastward over eastern China. Some of them ended in the East China Sea and coastal regions while others propagate further south.

Although the cold surge trajectories terminated around 30°N, the pressure, temperature, and meridional wind perturbations are observed further south. This is indicated in Fig. 6, the climatological evolution of cold surge associated SLP, temperature and northerly wind. For each winter (120 days, mid-November through mid-March), daily values of T3 are lag correlated with each of these fields. At each lag, the average correlation from all 16 winters is calculated. Since a cold surge is associated with a decrease in temperature the sign convention is such that: 1) a negative correlation with SLP indicates high pressure, 2) a positive auto-correlation with surface air temperature indicates low temperature, and 3) a positive correlation with the meridional wind indicates enhanced northerlies. Correlations for |r| 0.2 are contoured. This corresponds to the 95% confidence level for 100 independent time samples. While estimating the actual number of degrees of freedom is problematic, the correlation cutoff used is very conservative given that 120 time points in each of 16 years of data were used giving the potential of 1918 degrees of freedom ([16 x 120]-2).

At day -4, a massive high pressure covers most of Siberia, and temperatures are below normal. However, the signal in the meridional wind is weak at best. The centers of action in the surface air temperature and the SLP are located near Mongolia (95°E, 50°N) at this time. It is of interest to note the presence of

significantly below normal SLP in the vicinity of the maritime continent. This indicates the presence of a north-south gradient of SLP prior to the southward migration of the cold air and enhanced northerlies. Two days later, these centers of action have shifted southeastward, and the correlations have become stronger. The signal in the v-wind also strengthens, with the maximum northerlies located to the east of the SLP and temperature signals. By day 0 the cold air and pressure surge have spilled southward along the eastern flank of the Tibetan Plateau, with the strongest correlations located over region 3. By day +2 the cold surges have progressed further south, with the centers of action located over southeastern China. The signal in the v-wind is located even further south, with the strongest correlation (0.5) near 110°E, 5°N. Even on day +4, there still remains a close correspondence between the SLP and temperature centers, having now progressed to the southwest. The v-wind signature remains intact over the South China Sea, with the maximum correlation located on the equator at 105°E. The deeper intrusion of the northerlies into the tropics than either the SLP or temperature signature is a consistent feature during individual years, when the correlations may be even stronger.

The eastward extension is also a robust feature although may not appear as significant as the southward component. This is because the anticyclones that travel to the east, unlike those to the south, are subject to immediate and strong deformation by the warm and moist marine boundary once they reach the east coast. Cold surges that ended in the vicinity of the East China Sea belong to this category, and comprise a substantial number of total cold surges (see Fig. 5). The patterns of lag correlations of T2 with temperature, SLP and surface wind are found to be very similar to those presented in Fig. 6 (not shown).

The frequency, intensity, regionality, trajectory, and propagation patterns of the cold surges presented above have extended and substantiated the results of previous studies (Staff member of Academia Sinica, 1957; Zhu et al., 1981; Ding and Krishnamurti, 1987). They are also consistent with the annual cold surge summaries of BMC (1990).

Return to Table of Contents

4.3 Temporal distribution of cold surges and Siberian high

Figs. 7 (a) and (b) give the monthly cold surge events and the number of days that the Siberian high central pressure is greater than 1050 hPa. The intensity of the Siberian high tends to peak in December and January. However, the cold surge frequency exhibits maxima in November and March. This result contradicts with the well-accepted close relationship between the intensity of the Siberian high and occurrence of cold surges (Ding, 1994). Both dynamical and thermodynamical reasons can be attributed to this.

First, the East Asian large-scale flow is usually in a low-index mode during the regime transition period of November and March (Zhu et al., 1979). In December and January, however, the usual high-index large-scale flow is characterized by a strong Siberian high and an intense jetstream. This pattern is unfavorable for the occurrence of cold surges despite the abundance of cold air during this time. This is because that the short waves tend to move rapidly through such a pattern without causing any disturbances (Boyle, 1986a). The low index flow background, on the other hand, typically has a blocking over the Asian continent and deep troughing along the coast. This flow pattern yields a northwesterly flow over Lake Baikal which is highly unstable and more ready to release potential energy when triggered by a short wave (Boyle, 1986a).

Secondly, an important criterion of a cold surge is the 24-48 hour surface air temperature drop. During December and January, the jetstream is further south and the surface air temperature is relatively lower. As such, it takes a very strong anticyclone to induce a substantial temperature change in a cold background. While the surface air temperature is relatively warmer during November and March, cold air and anticyclones with modest intensity can significantly reduce the surface air temperature. From the view of weather forecasters, it is the cold surges that occur during November and March that yield a more abrupt temperature drop have the most significant damaging effect on local agriculture and economy.

Recently, a very similar monthly distribution of cold surges has been found by Ding and collaborators based on cold surges from 6 winters (Ding, personal communication, 1996). They suggest that the warm and moist troughs that moving out of the Bay of Bengal result in the relatively lower frequency cold surges during December and January.

As mentioned before, one of the necessary conditions of cold surge outbreak is that the Siberian high reaches a certain intensity. But this is by no means guarantee that the cold surge frequency should monotonically increase as the Siberian high intensifies. The statistics based on the 17-year data shown here and Ding's recent results do not support "The higher the Siberian high pressure, the greater the possibility of cold surge occurrence "(Ding, 1994), a statement that has been mistakenly known in the forecasting community.

The temporal distribution of strong cold surges is examined. Of all the 26 strong cases identified, 20 of them occurred in December, January and February, and five in November, only one in March and none during October or April. The strong cold surges tend to occur during very cold months. This suggests that large surface pressure gradient associated with a very strong surface anticyclone and abundant sources of cold air is an important driving force to push the cold air far into the tropics. This result also suggests that the intensity of the Siberian high may be related to the occurrence of strong cold surges that affect the tropical regions. Because the cold surge frequency is high in November and March and the prevailing northeasterly wind dominates a large area of East Asia during these months, November through March (NDJFM) should be the months for studying the East Asian winter monsoon and cold surges, rather than December through February (DJF) which the majority of winter monsoon studies has emphasized.

Return to Table of Contents

---

5. Interannual variation

In order to investigate the possible linkage between the interannual variation of the East Asian winter monsoon and ENSO, the 1979-1995 winter average Southern Oscillation Index is plotted in Fig. 8. Although the Southern Oscillation is not a standing phenomenon, the evolution of monsoon circulation during ENSO phases is ignored given that the winter monsoon is not examined on a monthly basis. The two major El Nino events of 1982/83 and 1986/87 exhibit low SOI. Negative departures of the SOI also occur during the 1989/90 and 1991/92 seasons. The 1988/89 La Nina event has SOI in excess of 2 hPa.

5.1 Cold surges

The annual cold surge frequency is first examined. An interesting feature in Fig. 9 is that minimum

frequency events occurs one year after the El Nino years. To test the robustness of this result, we investigated the sensitivity of the cold surge frequency to the SLP threshold in the cold surge definition. Aside from an expected decline in cold surge frequency with a stricter SLP criterion, the interannual variations were found to be insensitive. Further, the cold surge frequency from BMC during 1980-1984 shows the same variation pattern as in Fig. 9. Data from BMC also indicates that cold surge frequency reaches a minimum one year after the 1957/58 and 1965/66 El Nino events. This phenomenon agrees with the 1~1.5 year lag response of the northeast China surface air temperature to the SST near the eastern equatorial Pacific suggested by Bao et al. (1989).

As mentioned earlier, the definition of a cold surge is regionally dependent. The cold surges identified above, which are in good agreement with the observations from BMC, typically influence the bulk of East Asia and the coastal regions. However, a subset of these cold surges can reach to the South China Sea. This is illustrated in Figs. 10 (a) and (b), time series of meridional wind in three regions for the 1987/88 season, along with region 1 SLP. The phases of SLP variation are exactly reversed to those of region 3 meridional wind, which are followed chronologically by the similar variation patterns near Taiwan and in the vicinity of the South China Sea. The lags between the variation patterns in each region, which represent the southeast propagation of the surface anticyclones, are around 1-3 days.

The typical synoptic scenario of the propagation is as follows, before the outbreak of a cold surge, the intensification of the Siberian high simultaneously strengthens the northeasterly flow near region 3. The outbreak of the cold surge pushes the anticyclonic flow southeastward and increases the notherlies near Taiwan region. The wind then subsequently penetrated further into the northern part of the South China Sea and the cold surge ended. According to the weather forecasters (Li, personal communication, 1996) of Hainan Island (18°N, 110°E), whether a cold surge will affect the Island and the surrounding oceans depends on its path and intensity. When this region is under the influence of a cold surge, the most conspicuous weather phenomenon is the strong northeasterly wind. The seven strong wind events (northerly wind > 7 m/sec) near the South China Sea in the 1987/88 season, as indicated in Fig. 10 (a), is a subset of the eleven cold surges identified during the season. Strong wind events for other years are also examined (not shown). We found that, with on exception, every event is associated with a cold surge outbreak from the extratropics.

Because the surface meridional wind is the most important indicator of the cold surge activity in Hainan area, we define the South China Sea cold surge as the number of days that maximum northerly wind > 7 m/s in the region of (10°N-20°N,110°E-120°E). Similar definition has been used by Chang and Chen (1992). Based on this definition, the South China Sea cold surge frequency is shown in Fig. 11. The interannual variation of cold surge frequency is in good agreement with the pattern of SOI (correlation coefficient = 0.85). Low cold surge frequencies coincide with El Nino and low SOI events; high frequencies accompany with La Nina and high SOI years. This agrees with observed strong wind record of Hainan Island (Li, personal communication, 1996) for winters of 1950-1980, which indicates that cold air activity is much reduced during the years of 1957/58, 1965/66, 1968/69, and 1972/73, all are El Nino events.

Return to Table of Contents

5.2 Mean meridional wind

Frequency of the South China Sea cold surges not only bears good relationship with the SOI, but also largely controls the meridional wind variation over the South China Sea and over even larger areas. Fig. 12 shows time series of mean meridional wind for increasingly larger regions. The patterns in all the three regions are similar to that of the SOI. In agreement with the cold surges, stronger northerlies occur during La Nina and high SOI seasons, and weaker northerlies occur during El Nino and low SOI years. The correlation coefficient between the SOI and the meridional wind in the South China Sea (10°N-20°N,110°E-120°E) is 0.82. By examining the same time series as in Fig. 12 but over many nine-grid-point rectangular boxes near the western Pacific, we found that this SOI-like pattern of the wind does not exist in any of the areas outside the region of (0°N-20°N,100°E-130°E).

The meridional wind variation is a shallow phenomenon, occurring primarily at the surface. This is demonstrated in Fig. 13 where the wind variations near the South China Sea are plotted at the 925 hPa and 850 hPa levels. Although the patterns at both levels still bear certain resemblance to that of the SOI, the biennial oscillation is the dominant mode. At 700 hPa and above (not shown), the geostrophic flow is decidedly zonal over the entire East Asian continent and the wind in the northern part of the South China Sea is under great influence of the split jetstream south of the Tibetan Plateau. The signature of the SOI has been totally lost. Clearly, this SOI-like wind pattern is horizontally restricted within the region of (0°N-20°N,100°E-130°E) and vertically confined to the near surface layer.

Based on the above discussions, it is clear that the variation of area averaged meridional wind near the South China Sea and the maritime continent hinges on the variation of the South China Sea cold surges. The South China Sea cold surges share the same origin as the conventionally defined cold surges. The area averaged meridional wind near the South China Sea is thus greatly controlled by the northerlies propagated from the extratropics.

5.3 Large-scale features

As mentioned earlier, the surface Siberian high, 500 hPa trough, and the 200 hPa jetstream characterize the winter monsoon large-scale circulation and their strength are inherently related to each other.

Fig. 14 presents the number of days that the central pressure is greater than 1050 hPa in the region of (45°N-55°N, 90°E-110°E). Although this is not the only measure of the Siberian high intensity, the broad aspect of the interannual variation of this measure agrees with the SOI. The variation patterns indicate that, in general, the Siberian high is stronger (weaker) in La Nina (El Nino) and high (low) SOI years. The mean meridional wind averaged over the southeast periphery (5°N-20°N, 160°E-180°E) of the Siberian high, another way to represent the intensity of the high pressure, shows exactly the same result as that of Fig. 14 (not shown).

The variation of the 500 hPa geopotential height anomaly along 135°E is calculated. Although the overall variation pattern (not shown) is not comparable with the SOI, the 500 hPa trough is weaker during 1982/83, 1986/87 and 1991/92 El Nino events. The 200 hPa East Asian jet is also examined. Although this jet is subject to propagation or expansion in the east-west direction during different phases of ENSO, the jet intensity (at 140°E) is found abnormally weak during all three major El Nino events (not shown). This result is consistent with the weak Siberian high and 500 hPa trough.

Overall, the large-scale monsoon circulation is weaker than normal during all the three major El Nino events. In particular, the variation pattern of the Siberian high generally agrees with the SOI.

Return to Table of Contents

6. Summary and discussion

The study of the East Asian winter monsoon and cold surges from the 1979-1995 NCEP/NCAR reanalyses has revealed and extended several noteworthy climatological features of the winter monsoon. According to the conventional cold surge criteria, about 13 cold surges occur every winter season, of which two are strong cases that influence the tropical region. The average lifetime of the cold surges is about 7 days and the average intensity of highs is 1053 hPa. The strong cases usually last for about 9 days with average intensity of 1060 hPa.

The cold surges tend to originate from two source regions: one is near the northwest of Lake Baikal and the other is to the north of Lake Balkhash. The high pressure centers propagate southeastward, and end in the east and southeast of China and surrounding oceans. Consistent with trajectories of pressure centers, correlation patterns indicate that the signature of associated SLP, surface wind and surface air temperature stretches further south and east. The southward extent includes the bulk of the maritime continent; the eastward extent reaches 150°E.

Although the intensity of the Siberian high varies according to the season and reaches its peak in January, the cold surges are most active during November and March.This result suggests that November through March should be considered as the East Asian winter monsoon season. It also indicates that the occurrence of cold surges does not monotonically increase with the strengthening of the Siberian high, an empirical rule that has been widely believed in the forecasting community. Examination of monthly distribution of strong cold surges indicates, however, that the majority of strong cold surges occurs during DJF. This result suggests that large pressure gradient associated with strong Siberian high is an important driving force to push the cold air far into the tropics.

The two stratifications of cold surges are revealing when considering the relationship between ENSO and the interannual variation of the cold air activity. The first stratification, as described in the cold surge identification criteria, yields result that is consistent with the in situ observation from BMC. The interannual variation of cold surge frequency shows that minimum surge frequency occurs one year after an El Nino event. The second stratification, based on the maximum meridional wind event in the South China Sea, indicates that the interannual variation of the South China Sea cold surge is in good agreement with the SOI. High cold surge frequency is found during La Nina and high SOI events, low frequency is associated with El Nino and low SOI events.

The variation of the mean meridional wind near the South China Sea and tge narutune hinges on the South China Sea cold surges. As in the case of the cold surges, the interannual variation of the wind is also well correlated with the SOI. Strong wind years are associated with La Nina and high SOI events; weak wind years are found during El Nino and low SOI events. This pattern of variation is restricted north of the equator within (0°N-20°N,100°E-130°E), and confined to the near surface layer. The interannual variation of the Siberian high, measured by means of both pressure and wind, is in general agreement with the SOI. Both the strength of the 200 hPa jetstream and the 500 hPa trough are found to be weaker than normal during El Nino events, although their interannual variation patterns do not agree with the SOI as closely as that of the Siberian high.

Given the close relationship between the SOI and the interannual variation of the monsoon meridional

wind and cold surges, it is natural to wonder why some of the monsoon related disturbances, either originated from or located in the extratropics, exhibit variation patterns similar to the SOI, and what are the physical mechanisms between the ENSO/winter monsoon interaction.

During a typical El Nino year, the convective activity in the maritime continent is usually reduced. If the cumulus convection in this region is one of the most important monsoon energy sources as suggested by Ramage (1971), the suppression of the maritime convection should be responsible, at least partly, for the weaker than normal extratropical monsoon circulation during El Nino events. With the available observed outgoing longwave radiation (OLR) data from the National Oceanic and Atmospheric Administration, we have computed the OLR anomaly in the maritime continent (110°E-120°E, 5°N-5°S) from 1979-1992. The overall interannual variation pattern (not shown here) is not as close to the SOI as that of the South China Sea cold surges or the Siberian high. However, negative anomaly is found during the 1988/89 La Nina season; likewise, positive OLR anomalies are found during the 1982/83 and 1986/87 El Nino seasons. The correlation coefficient between the OLR anomaly and the SOI is $|R|=0.5$.

On the other hand, evidence indicated that the winter monsoon and cold air activity can greatly affect the tropical convective activity and SST. Slingo (1996, personal communication) found that Indonesian convection is enhanced when cold surges penetrated far into the tropics. Chang et al. (1979) have shown that cold surges are capable of influencing the tropical SST. But whether the cold surges can significantly affect the tropical region, as has been discussed, depends on the intensity and path of the cold surges. It may also relate to the background large-scale circulation. Theoretical studies have suggested (Branstator 1983, Lau and Lim 1984) that the interaction between the tropical convection and midlatitude circulation depends critically on the relative position of the convection and extratropical quasi-stationary waves. It has also been suggested that the interaction between cold surges and convective activities near the maritime continent will in turn modify the extratropical and tropical synoptic and planetary scale circulations (Chang and Lau, 1980). Apparently, further studies are much needed to delineate the mechanism of the interaction between the winter monsoon and convection near the maritime continent.

In summary, in addition to extend and substantiate the climatological aspects of the East Asian winter monsoon and cold surges, the current study has clearly indicated that the interannual variation of the South China Sea cold surges is in good agreement with the SOI. The South China Sea cold surges share the same origin with the conventionally defined cold surges. They also dominate the variation of the area averaged meridional wind near the South China Sea and the western Pacific. The conventionally defined cold surges, on the other hand, reached minimum frequencies one year after El Nino events. Large-scale monsoon circulations are found to be weaker than normal during El Nino years. However, physical mechanisms responsible for the interaction between ENSO and the winter monsoon are still not well understood, especially problems on if and how the winter monsoon cold air activity affects the ENSO through its impact on tropical SST pattern and convective activities in the maritime continent. Simulations of coupled ocean models and GCM simulations with specified observed SST, such as simulations from the Atmospheric Model Intercomparison Project (AMIP), should provide a good opportunity to address these problems.

Return to Table of Contents

Acknowledgments

We wish to thank Yihui Ding of National Climate Center, China for helpful discussions and sharing his yet-to-be-published results, and Y.-L. Zhang and S.-J. Chen of Peking University, China for providing the observed cold surge data. Tian-Fu Li of Hainan Meteorological Bureau provided valuable information and offered his forecasting experience. Michael Fiorino facilitated access to the NCEP/NCAR reanalysis. This work was performed under the auspices of the U.S. Department of Energy Environmental Science Division at the Lawrence Livermore National Laboratory under contract W-7405-ENG-48.

References

Bao, C.-L., S.-M. Xie, and D.-Y. Wei, 1989: The East Asian winter monsoon and El Nino event. Preprint, US/PRC Monsoon Workshop, University Park, PA. The Pennsylvania State University. 23-25.

Beijing Meteorological Center, 1990: Annual cold surge summary. BMC internal report. [Available from Data Processing Center, Beijing Meteorological Center, Beijing, 100871, China]

Boyle, J. S., 1986a: Comparison of the synoptic conditions in midlatitude accompanying cold surges over the Eastern Asia for the months of december 1974 and 1978. Part 1: monthly mean fields and individual events. Mon. Wea. Rev., 114, 903-918.

Boyle, J. S., 1986b: Comparison of the synoptic conditions in midlatitude accompanying cold surges over the Eastern Asia for the months of december 1974 and 1978. Part 2: relation of surge events to features of the longer term mean circulation. Mon. Wea. Rev., 114, 919-929.

Boyle, J. S., and C.-P. Chang, 1984: Monthly and seasonal winter climatology over the global tropics and subtropics for the decade 1973-1983. Report NPS-63-84-006, 30pp. [Available from Naval Postgraduate School, Monterey, CA, 93943]

Boyle, J. S., and T.-J. Chen, 1987: Synoptic aspects of the wintertime East Asian monsoon. Monsoon Meteorology. C.-P. Chang and T. N. Krishnamurti, Eds., Oxford Univer. Press. 125-160.

Branstator, G., 1983: Horizontal energy propagation in a barotropic atmosphere with meridional and zonal structure. J. Atmos. Sci., 40, 1689-1708.

Chang, C.-P., and K.-M. Lau, 1980: Northeasterly cold surges and near-equatorial disturbances over the Winter MONEX area during December 1974. Part 2: Planetary-scale aspects. Mon. Wea. Rev., 108, 298-312.

Chang, C.-P., and K.-M. Lau, 1982: Short-term planetary scale interaction over the tropics and the mid-latitudes. Part 1: contrast between active and inactive period. Mon. Wea. Rev., 110, 933-946.

Chang, C.-P., and J. M. Chen, 1992: A statistical study of winter monsoon cold surges over the South China Sea and the large-scale equatorial divergence. J. of Meteo. Soc. of Japan, 70-1, 287-302.

Chang, C.-P., J. Erickson, and K.-M. Lau, 1979: Northeasterly cold surges and near-equatorial disturbances over the winter-MONEX area during 1974. Part 1: Synoptic aspects. Mon. Wea. Rev., 107, 812-829.

Ding, Y. H. 1994: Monsoon over China. Kluwer Academic Publishers, 432pp.

Ding, Y. H. and T. N. Krishnamurti, 1987: Heat budget of the Siberian high and the winter monsoon.

Mon. Wea. Rev., 115, 2428-2449.

Kalnay, E., M. Kanamitsu, R. Kistler, W. Collins, D. Deaven, L. Gandin, M. Iredell, S. Saha, G. White, J. Woollen, Y. Zhu, M. Chelliah, W. Ebisuzaki, W. Higgins, J. Janowiak, K. C. Mo, C. Ropelewski, J. Wang, A. Leetmaa, R. Reynolds, R. Jenne, and D. Joseph, 1996: The NCEP/NCAR 40-year reanalyses project. Bull. Ame. Meteor. Soc., 77, 437-471.

Lau, K.-M., and C.-P. Chang, 1987: Planetary scale aspects of the winter monsoon and atmospheric teleconnections. Monsoon Meteorology. C.-P. Chang and T. N. Krishnamurti, Eds., Oxford Univer. Press. 161-201.

Lau, K.-M., and M.-T. Li, 1984: The monsoons of East Asia and its global associations - a survey. Bull. Ame. Meteor. Soc., 65, 114-125.Lau, N.-C., and K.-M.

Lau, K.-M., 1984: The structure and energetics of midlatitude disturbances accompanying cold-air outbreaks over East Asia. Mon. Wea. Rev., 112, 1309-1327.

Pan H.-M., X. Jia, and X.-Z. Young, 1985: The climatological features of outbreaks of cold air in China. Paper collection of Beijing Meteorological Center, CMA. 120-131. [Available from Beijing Meteorological Center, Beijing, 100871, China]

Ramage, C. S.,1971: Monsoon Meteorology, Academic Press, 296pp.

Staff members, Academia Sinica 1958: On the general circulation over eastern Asia. 2. Tellus, 10, 58-75.

Zhang, Y., and W.-C. Wang, 1996: GCM simulated northern winter cyclone and anticyclone activity under a greenhouse warming scenario. J. of Climate, (in revision)

Zhu, Q.-G., J.-L. Lin, and S.-W. Shou, 1981: Theory and Method of Synoptic Meteorology. Beijing Meteorological Press, 535pp.

Return to Table of Contents
Return to PCMDI Reports Series Page

For further information about this report, please contact Tom Phillips (phillips14@llnl.gov).
This site is maintained by Anna McCravy mccravy1@llnl.gov.

Last updated November 13, 2000.


and LLNL Disclaimers

UCRL-ID-125332

Fig. 1. The averaged East Asian mean sea-level pressure superimposed on the surface (10 meter) wind for winter (DJF) of 1979/80-1994/95. Unit: hPa and ms-1.

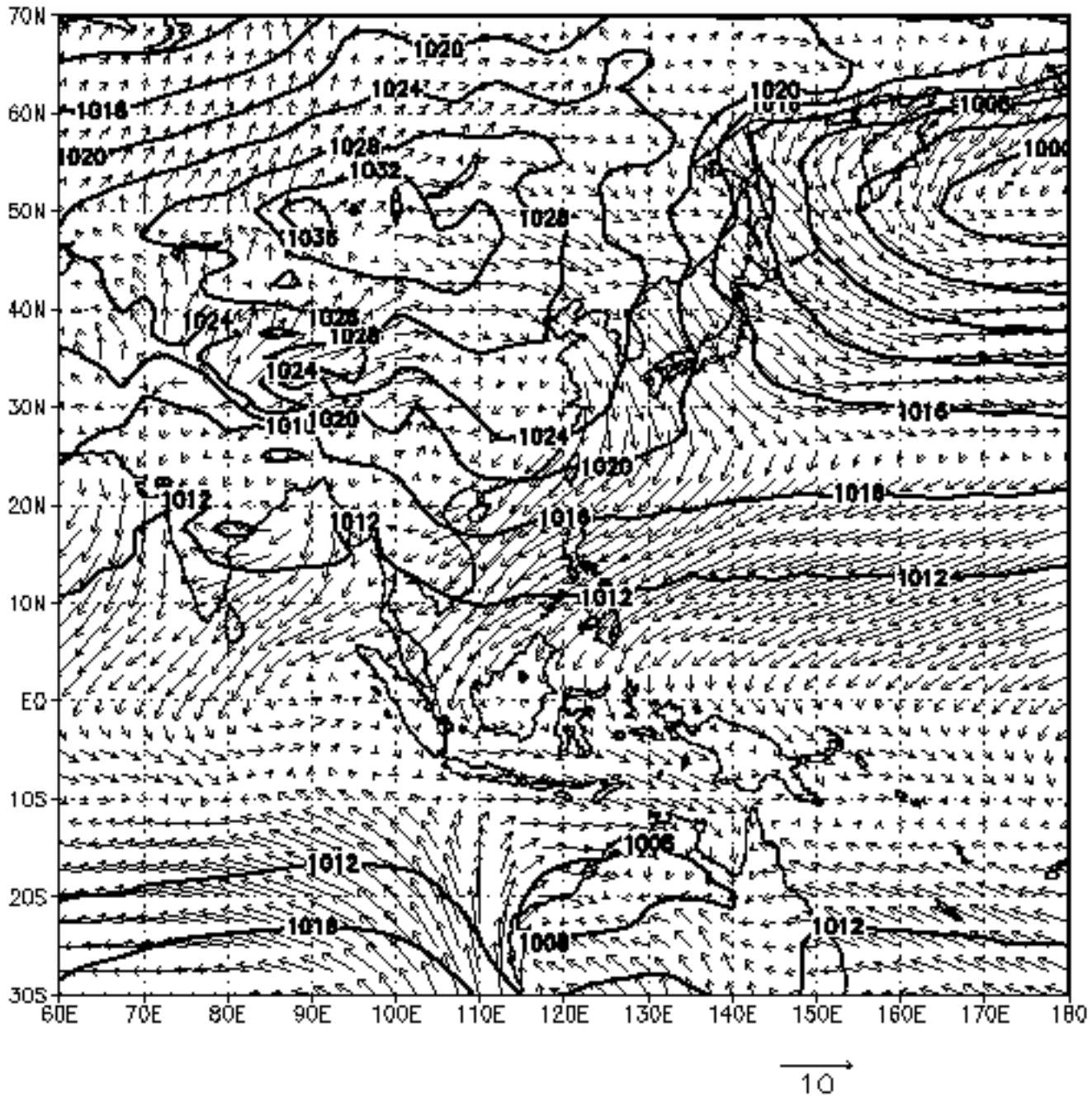

Fig. 2. (a) upper-left, standard deviation of sea-level pressure averaged from November to March of 1979/80-1994/95. Unit: hPa (b) upper-right, same as in (a) except for the surface air temperature (2m). Unit: °C (c) lower-left, percent of total SLP variance explained by periods of 6-14 days averaged from November to March of 1979/80-1994/95. (d) lower-right, same as in (c) except for the surface air temperature (2m).

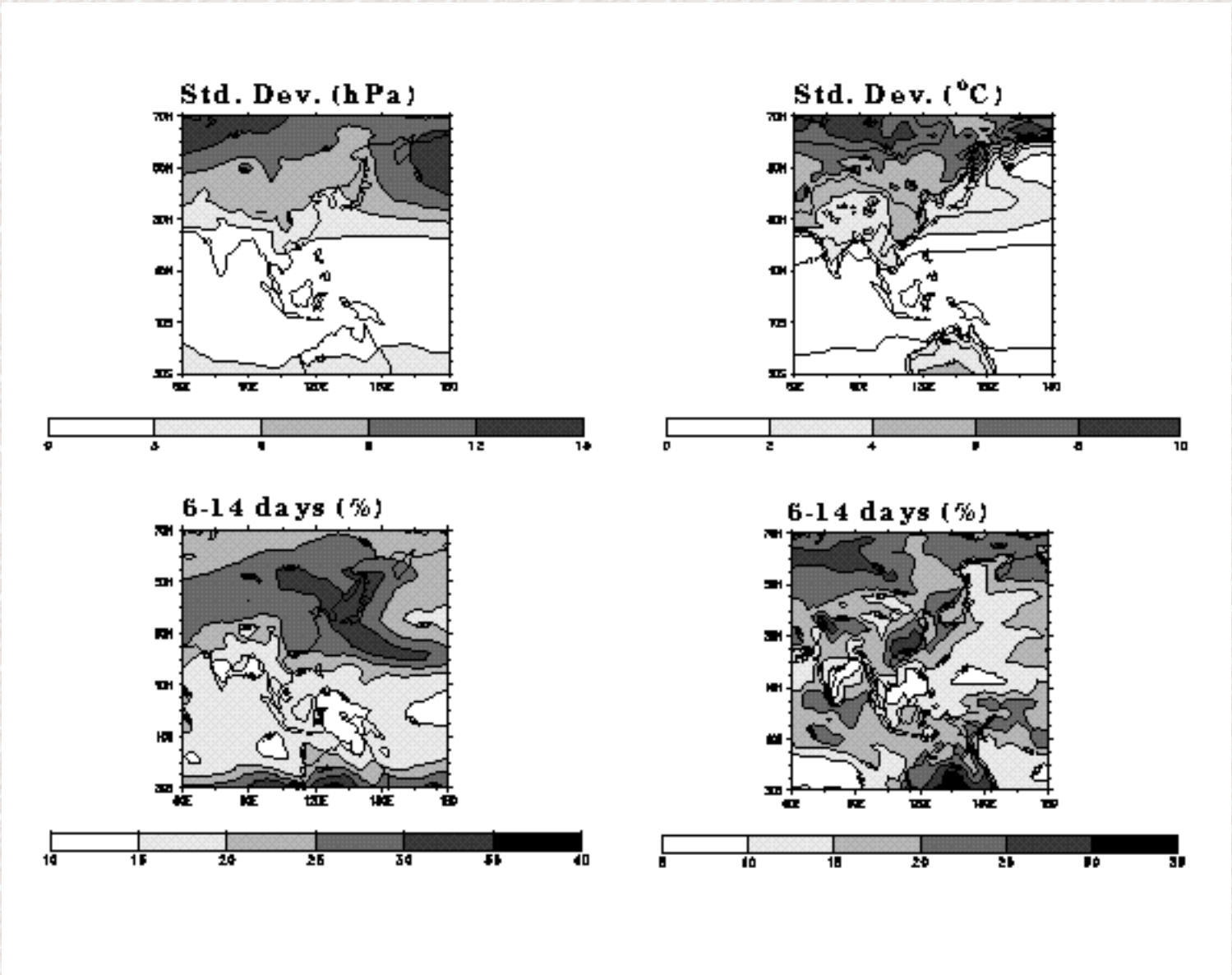

Fig. 3. Selected sub-areas for cold surge identification in the East Asian region. The size of each area is 5° latitude x 5° longitude.

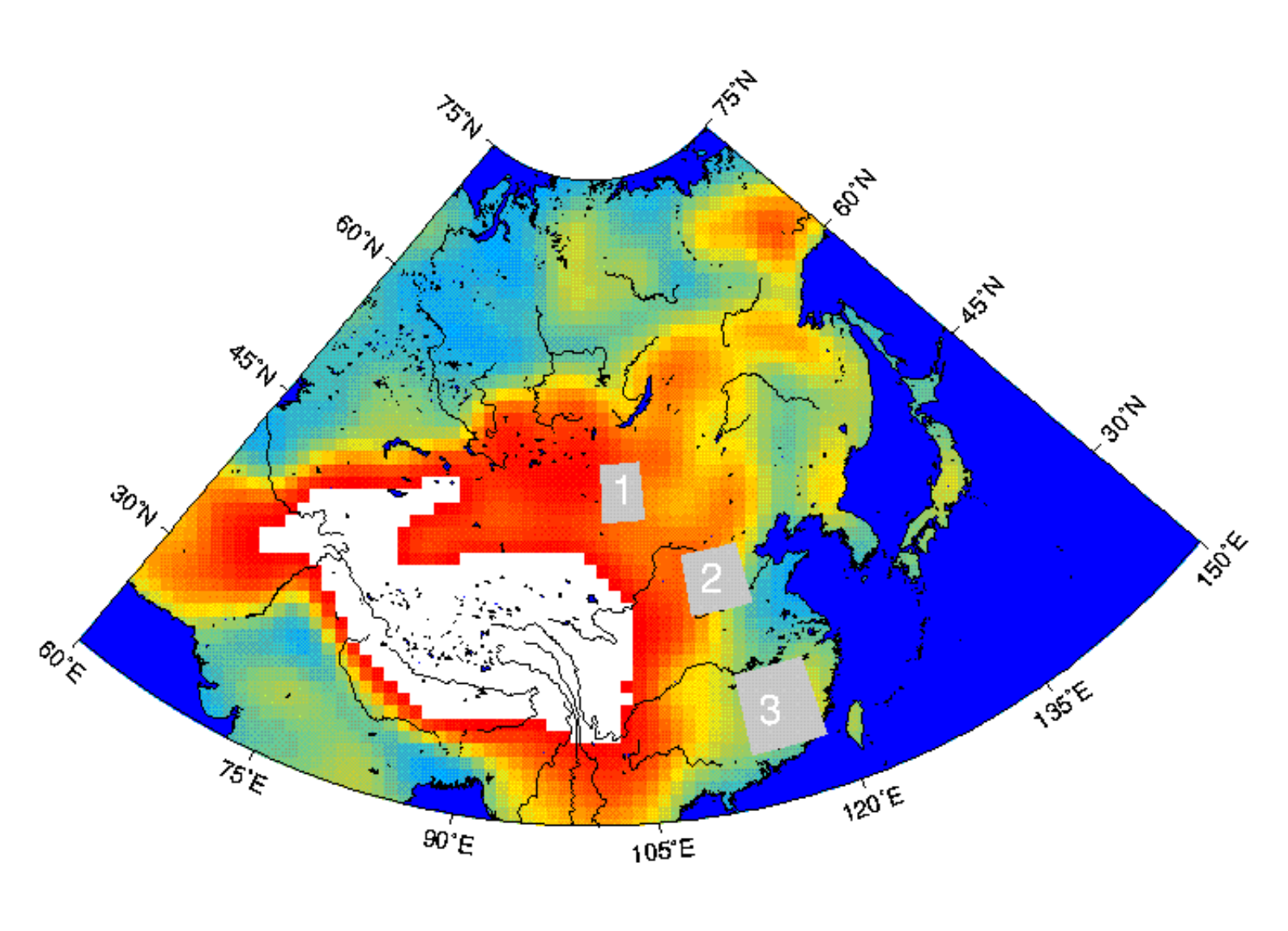

Fig. 4. Twice daily time series of surface air temperature (2m) over region 1,2 and 3 from November of 1987 to March of 1988. A five-point running average has been applied. Unit: °C.

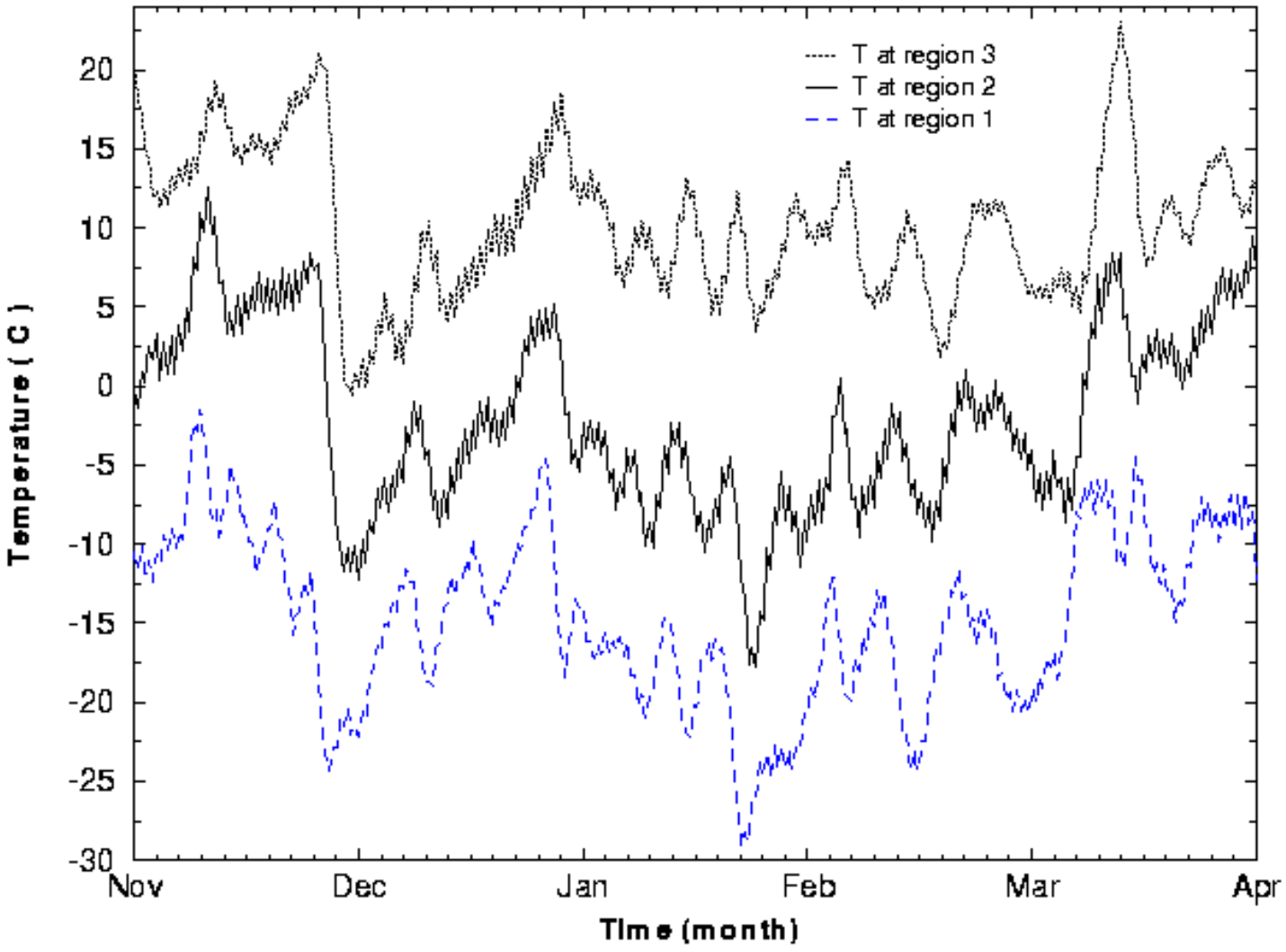

Fig. 5. Trajectories of the surface anticyclones associated with all cold surges for the period October-April of 1979/80 - 1994/95. The origin of the cold air and the ending of the surges are denoted in circles and squares, respectively.

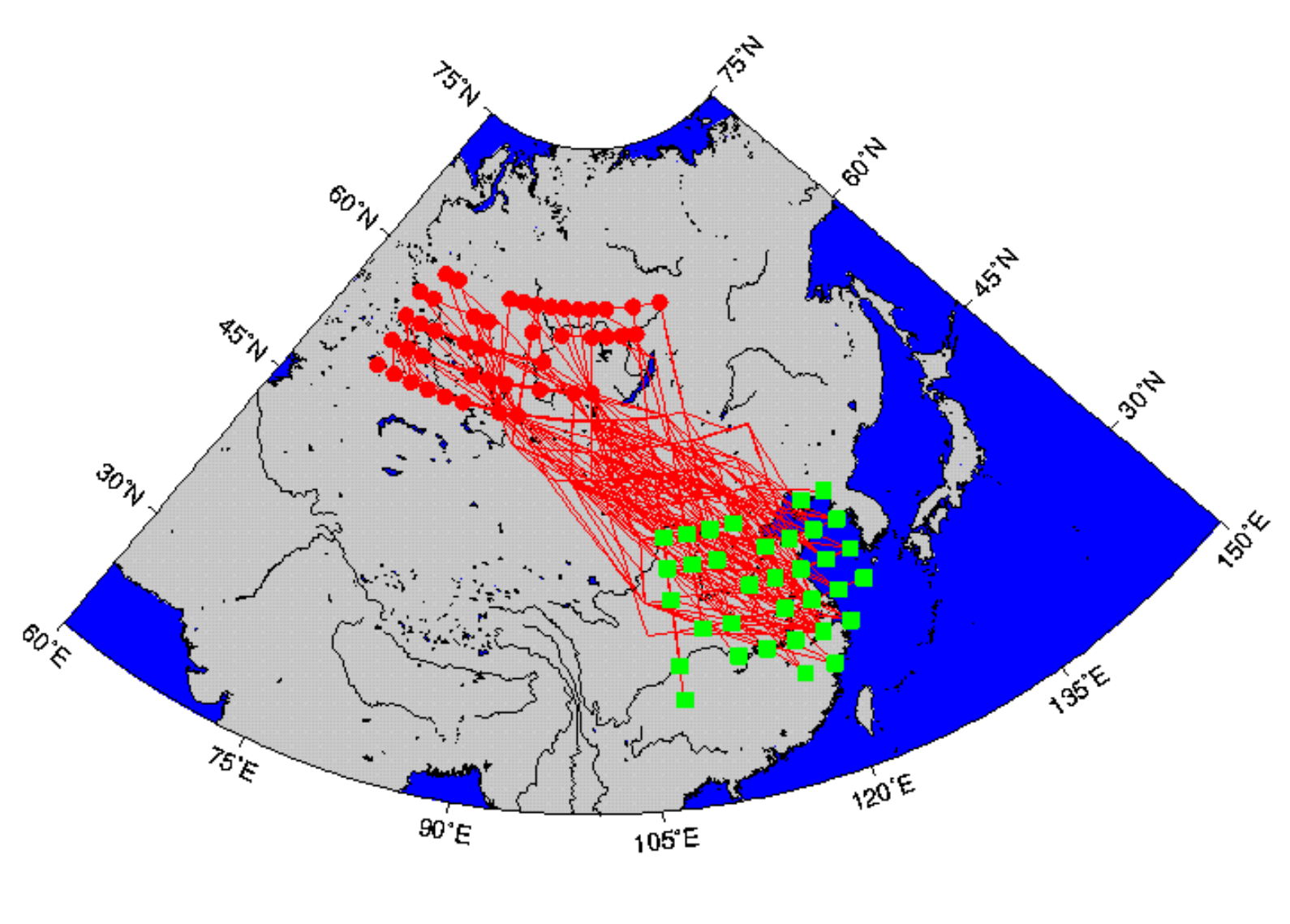

Fig. 2. (a) upper-left, standard deviation of sea-level pressure averaged from November to March of 1979/80-1994/95. Unit: hPa (b) upper-right, same as in (a) except for the surface air temperature (2m). Unit: °C (c) lower-left, percent of total SLP variance explained by periods of 6-14 days averaged from November to March of 1979/80-1994/95. (d) lower-right, same as in (c) except for the surface air temperature (2m).

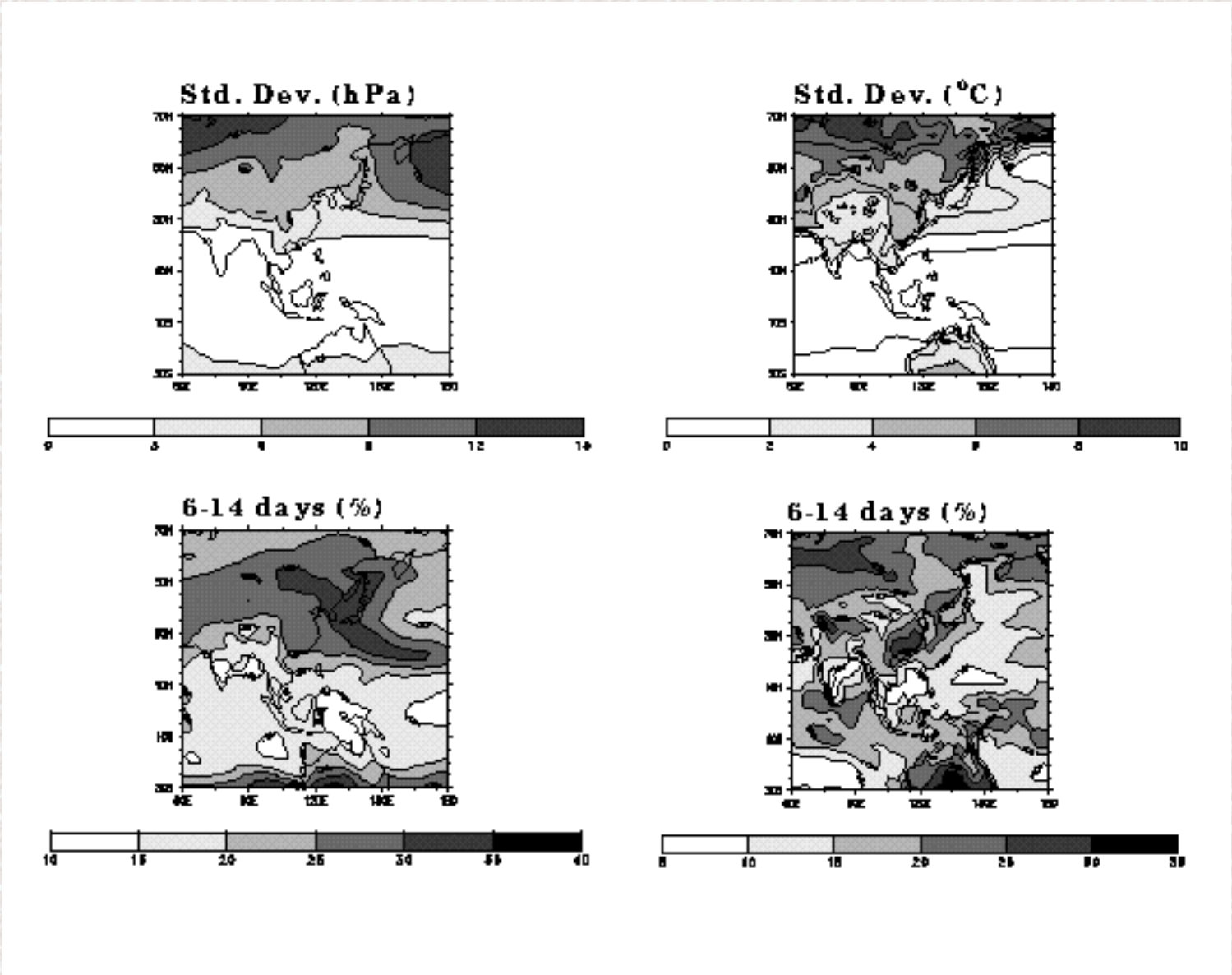

Fig. 3. Selected sub-areas for cold surge identification in the East Asian region. The size of each area is 5° latitude x 5° longitude.

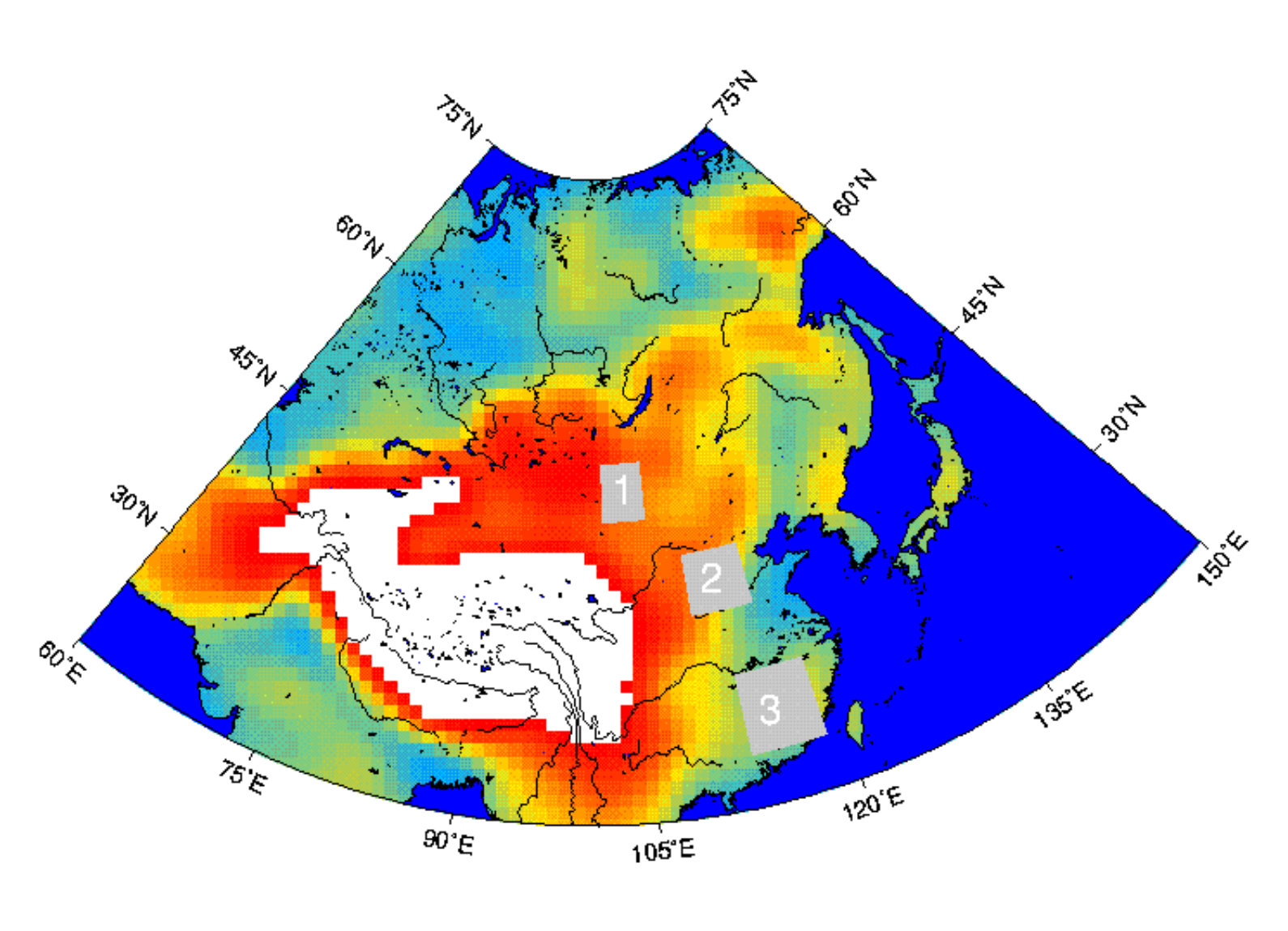

Fig. 4. Twice daily time series of surface air temperature (2m) over region 1,2 and 3 from November of 1987 to March of 1988. A five-point running average has been applied. Unit: °C.

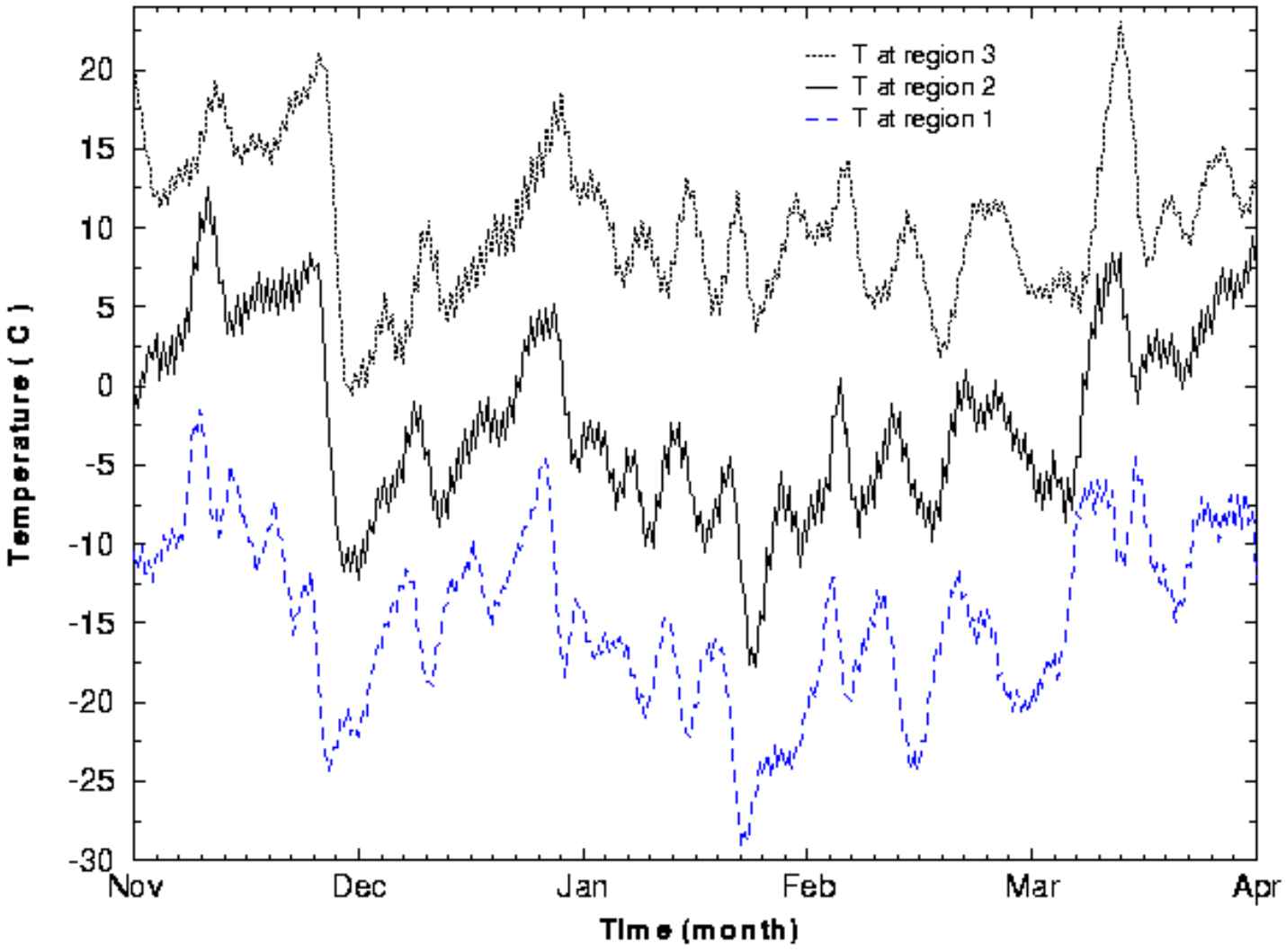

Fig. 6. Average lag correlations of region 3 surface air temperature with sea level pressure, surface air temperature, and surface v-wind (10m) for the period mid-November through mid-March for 1979/80-1994/95. Positive (negative) correlations ≥ 0.2 (≤ -0.2) are shaded white (black). For sea level pressure, negative correlations are plotted for R ≤ -0.2 at an interval of 0.1. For surface air temperature and v-wind, positive correlations are plotted for R 0.2 at an interval of 0.1. The use of $|R| \geq 0.2$ corresponds to the 95% confidence level for 100 degrees of freedom.

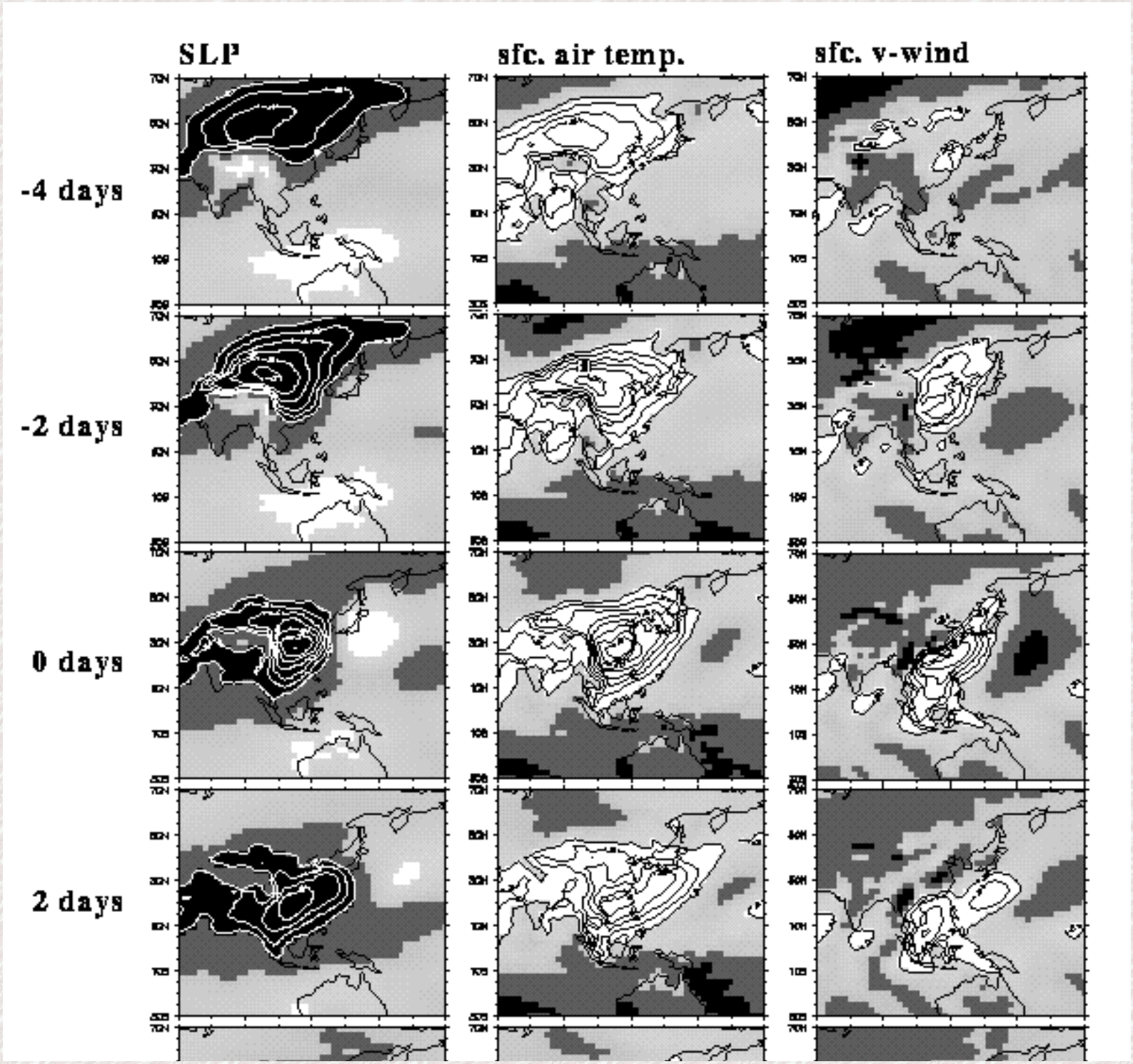

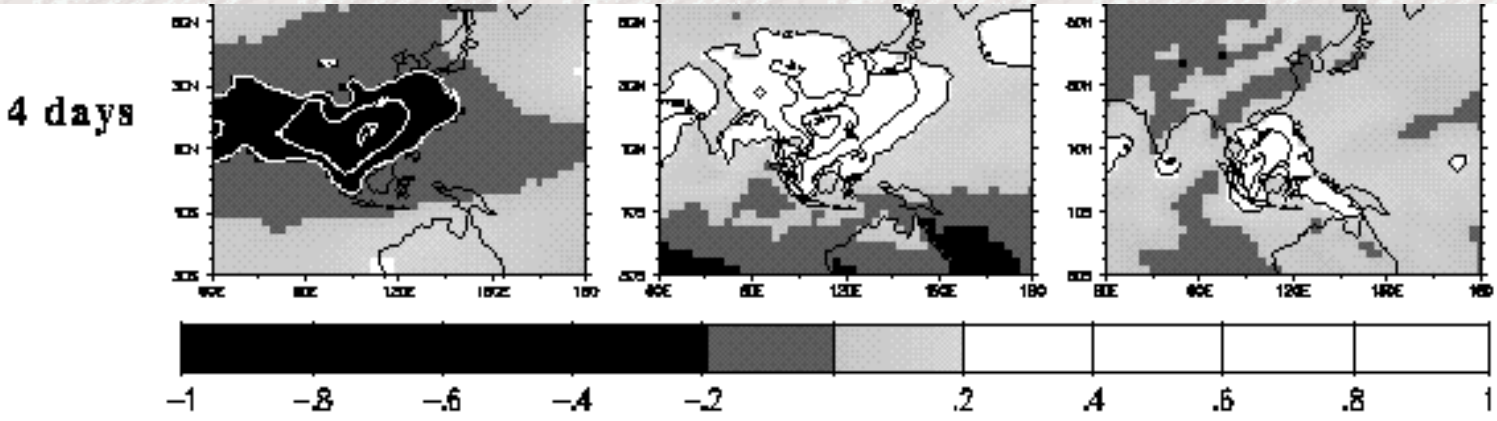
4 days
−1
−.8
−.6
−.4
−.2
.2
.4
.6
.8
1

Fig. 7. (a) Monthly distribution of number of cold surges. These variables are for the period of October - April of 1979/80-1994/95.

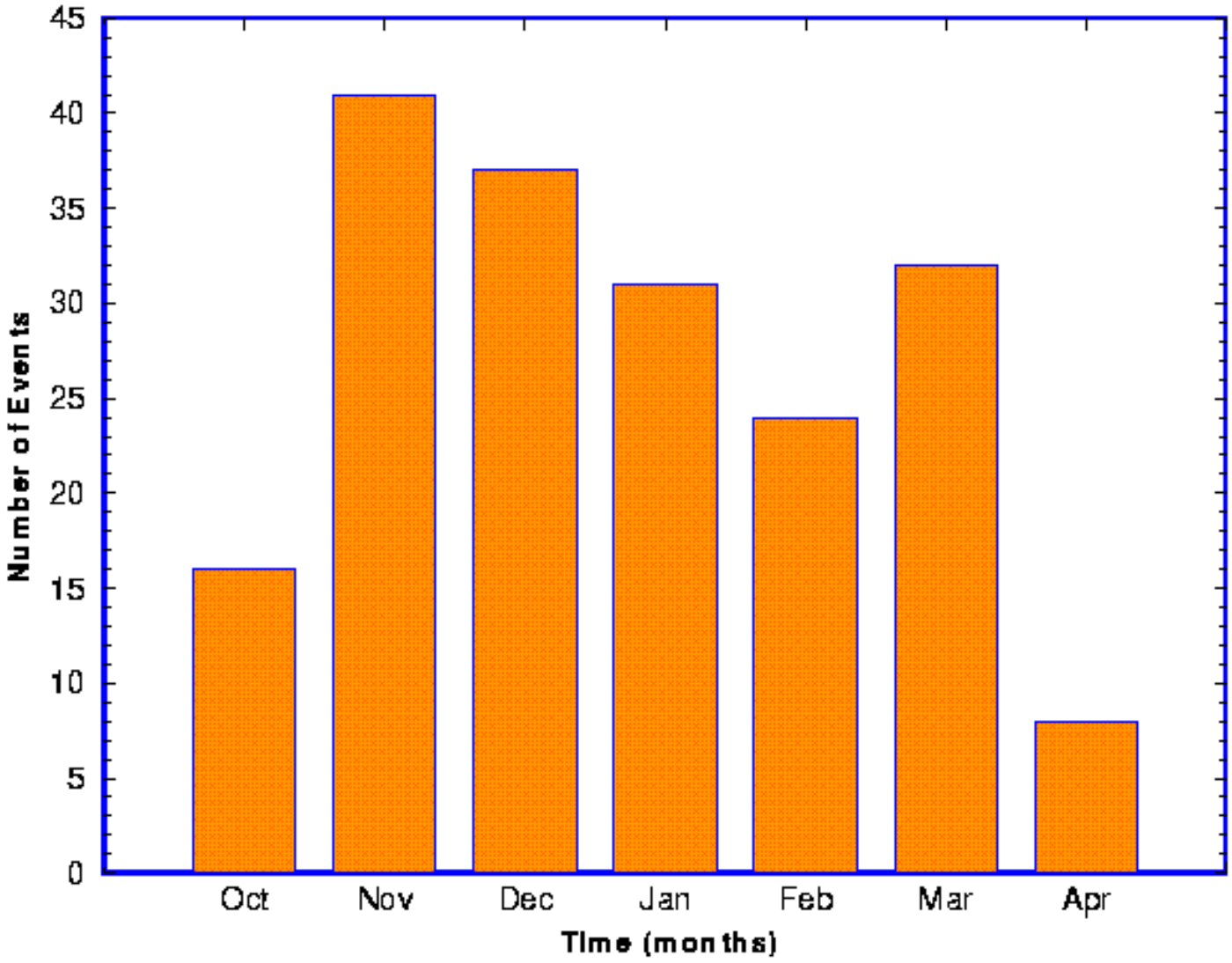

Fig. 7. (b) Monthly distribution of number of days that the Siberian high exceed 1050 hPa. These variables are for the period of October - April of 1979/80 - 1994/95.

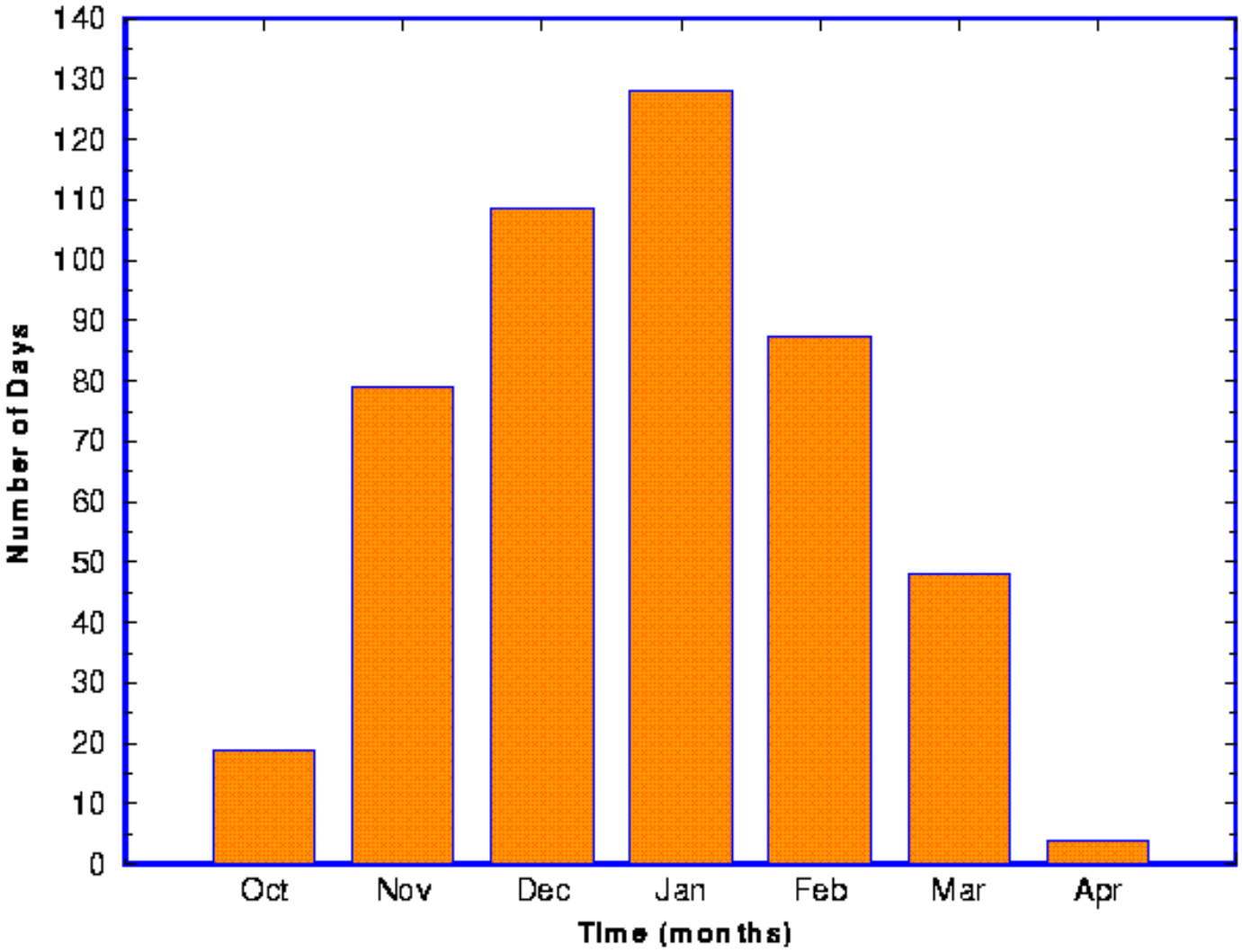

Fig. 8. Seasonal (NDJFM) averaged Southern Oscillation Index. Anomaly of pressure difference between Tahiti and Darwin. Unit: hPa. The year 1980 in the x-axis represents the winter of 1979/80 and so on. This applies to all the figures for interannual time series shown below.

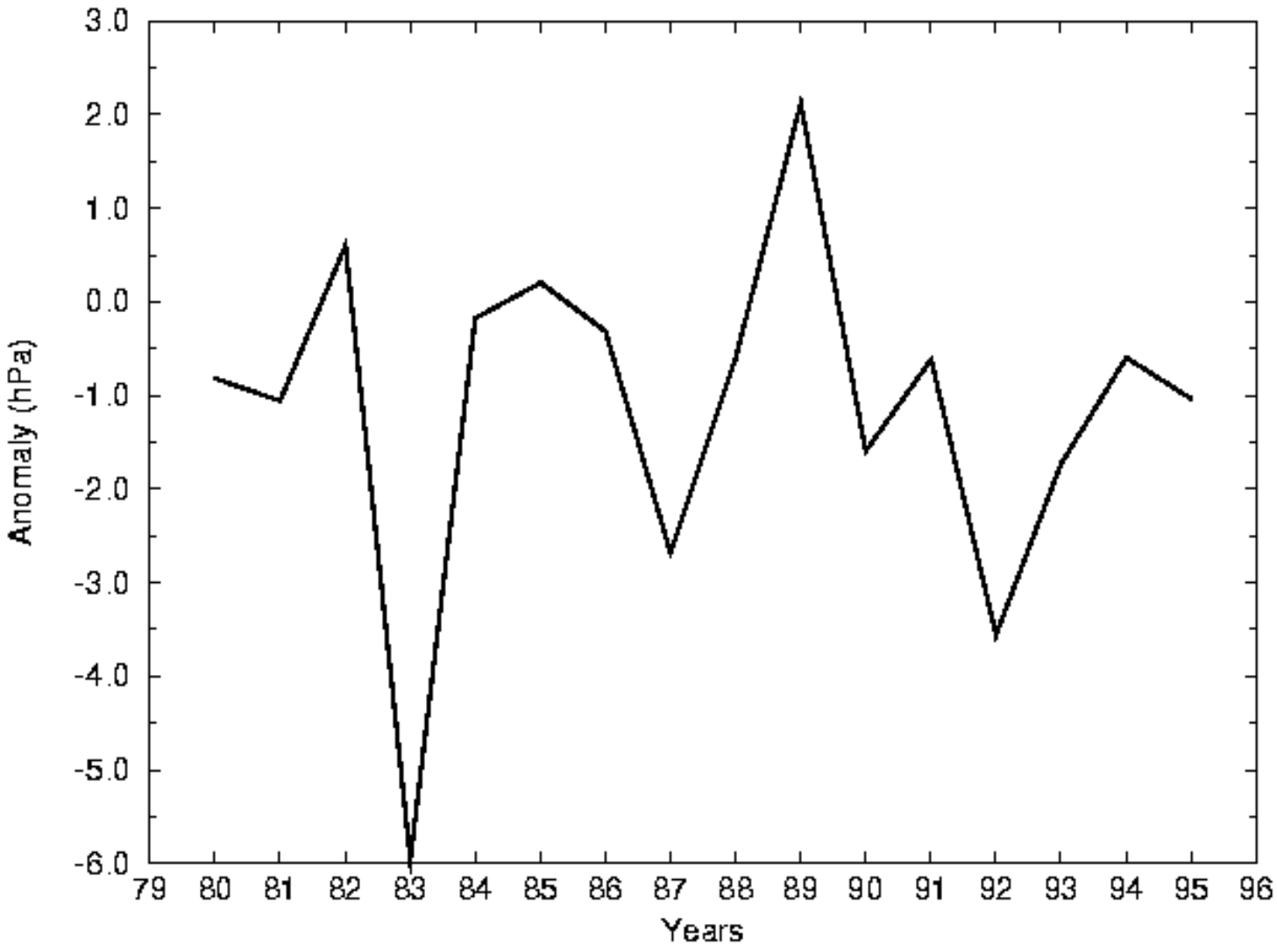

Fig. 9. Cold surge frequency from 1979/80-1994/95. Unit: number of events per season.

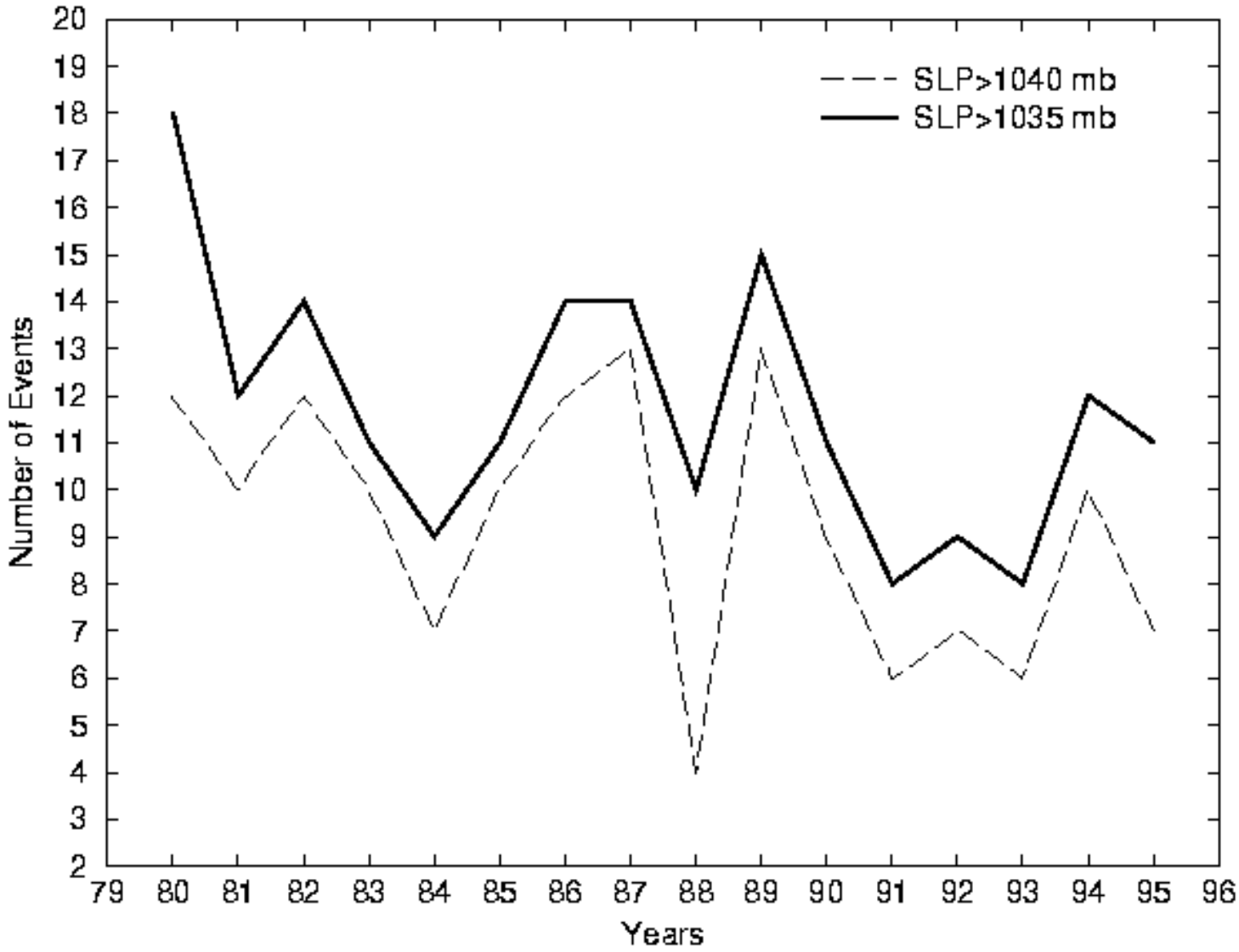

Fig. 10. (a) Twice daily time series of area averaged meridional wind from region 3, near Taiwan (120°E-125°E; 22.5°N-27.5°N), and in the vicinity of the South China Sea (110°E-115°E; 10°N-20°N). Unit: m/sec.

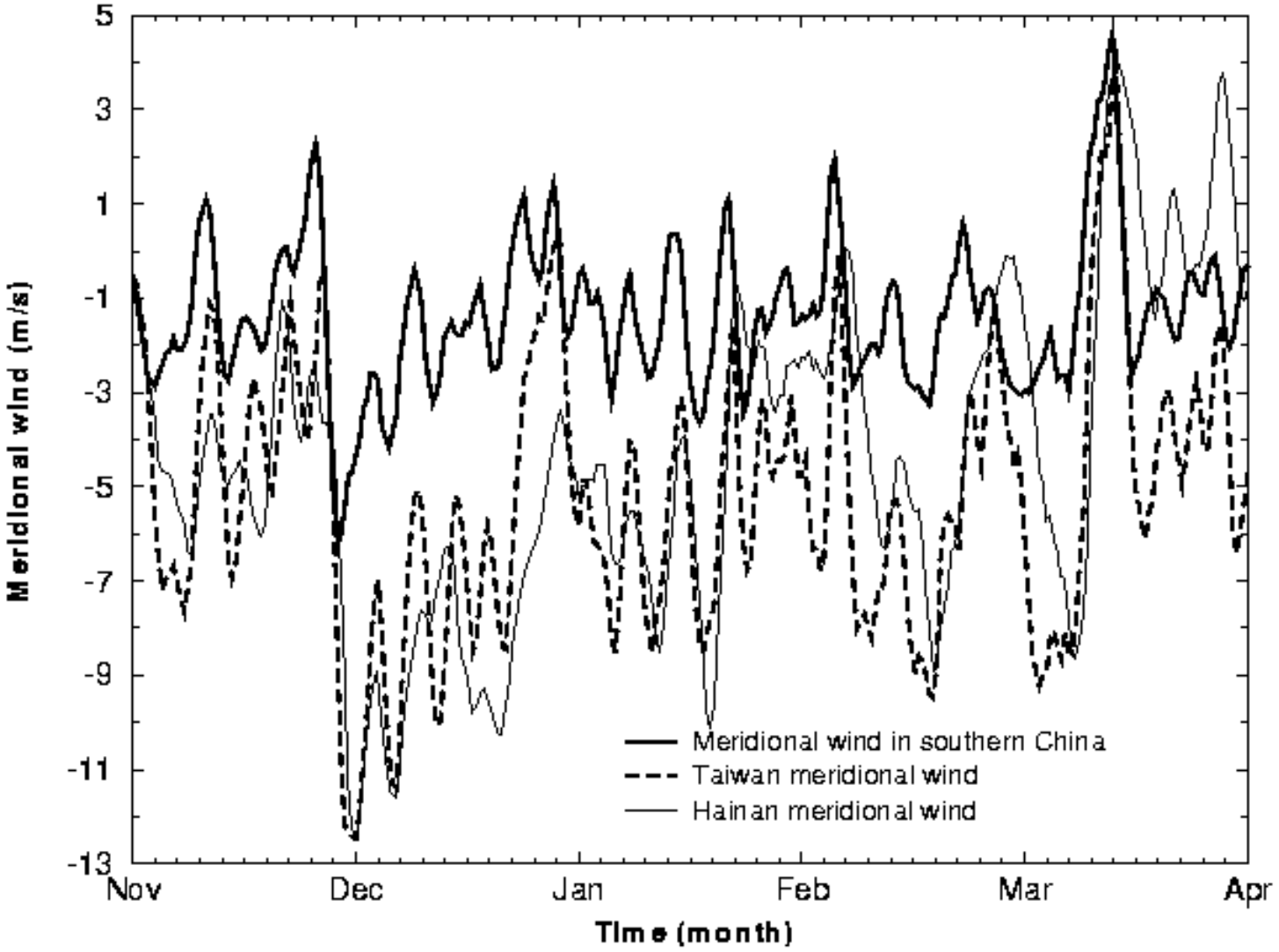

Figure 10. (b) Twice daily time series of region 1 SLP from November of 1987 to March of 1988. Unit: hPa. A five-point running average has been applied to all the fields.

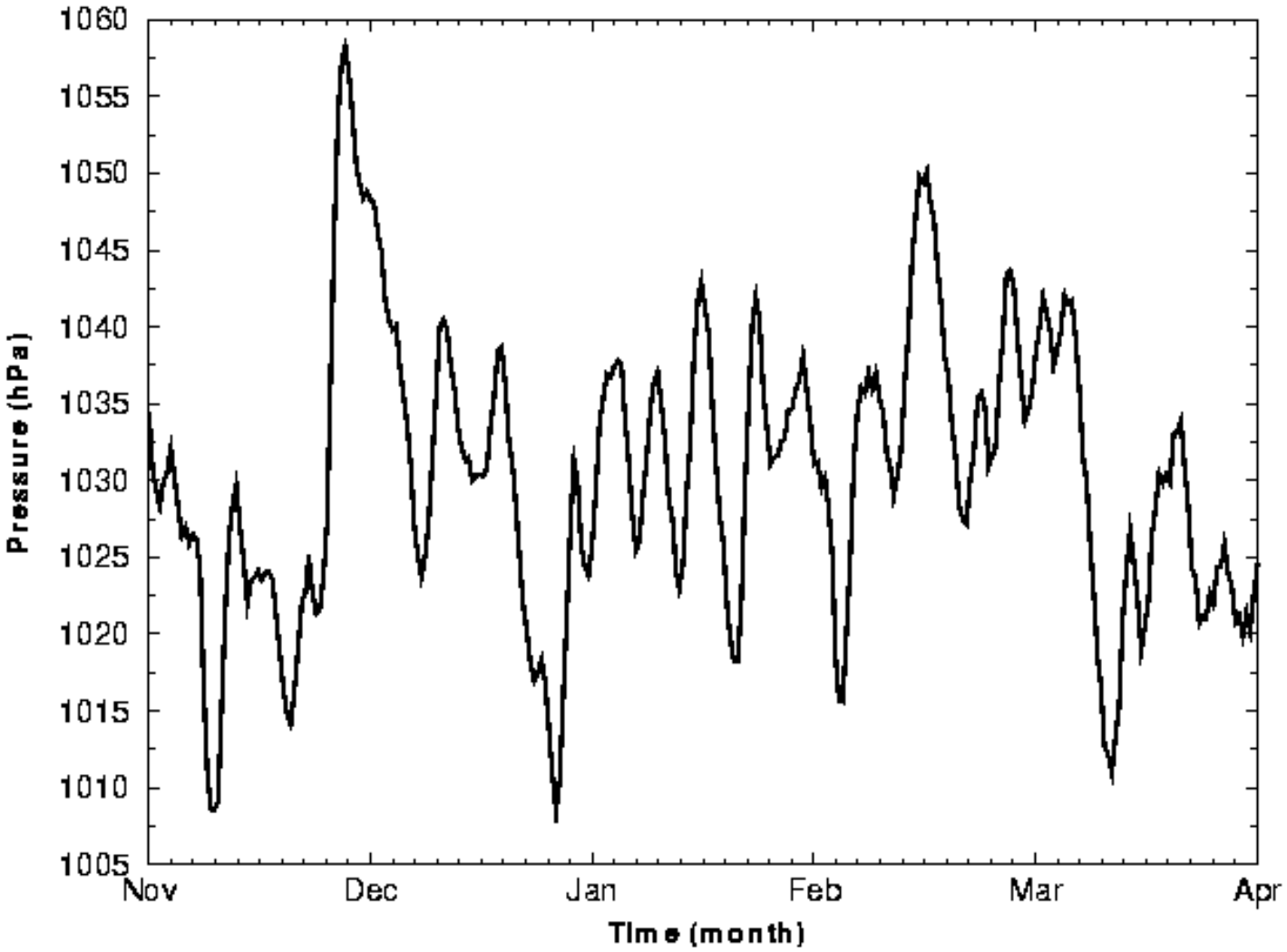

Fig. 11. Cold surge frequency in the South China Sea, number of days the maximum northerly wind near the South China Sea (110°E-120°E; 10°N-20°N) exceed 7 m/s. Unit: number of days per season.

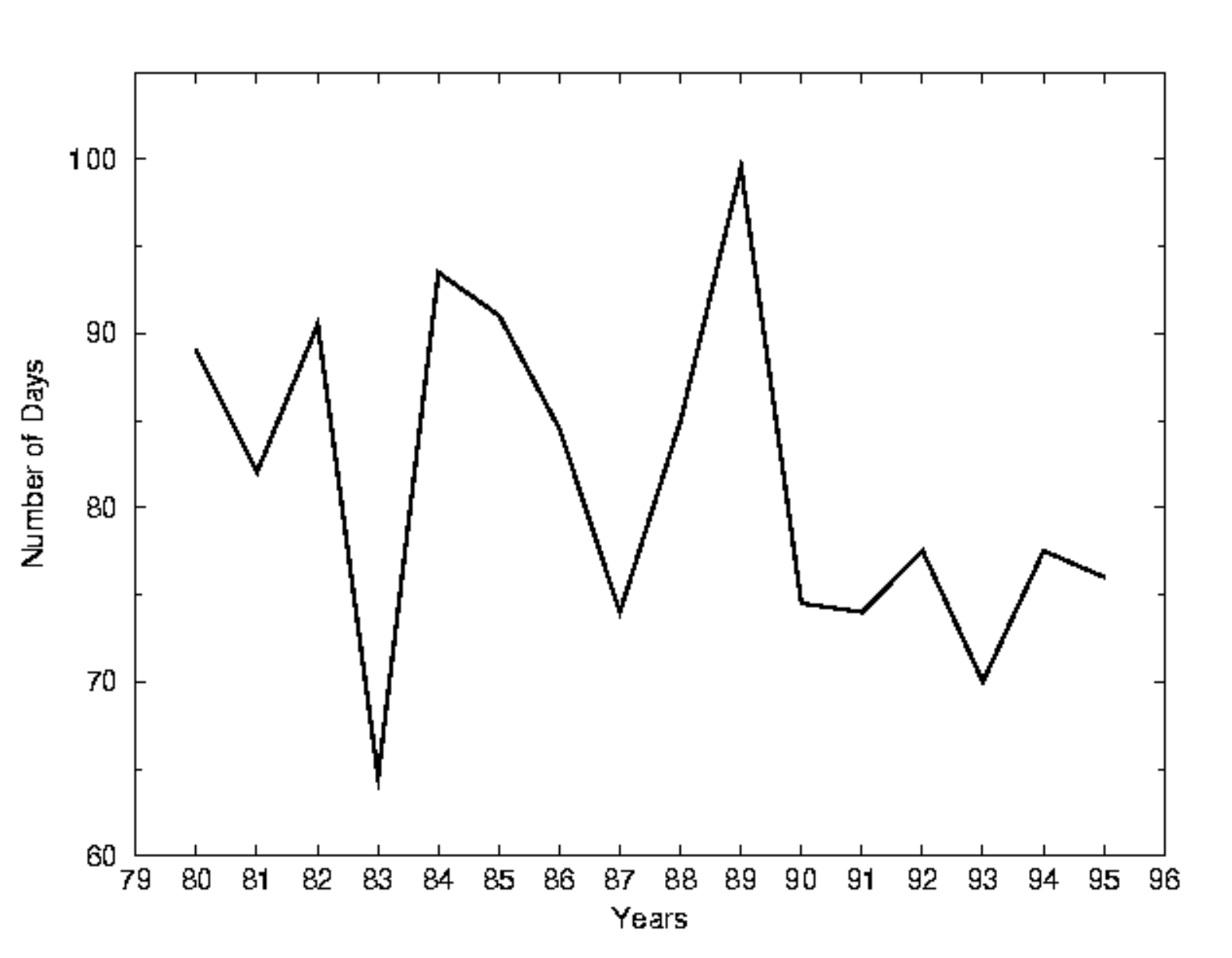

Fig. 12. Winter (NDJFM) area averaged northerly wind over three regions near the South China Sea and western Pacific. Unit: m s-1.

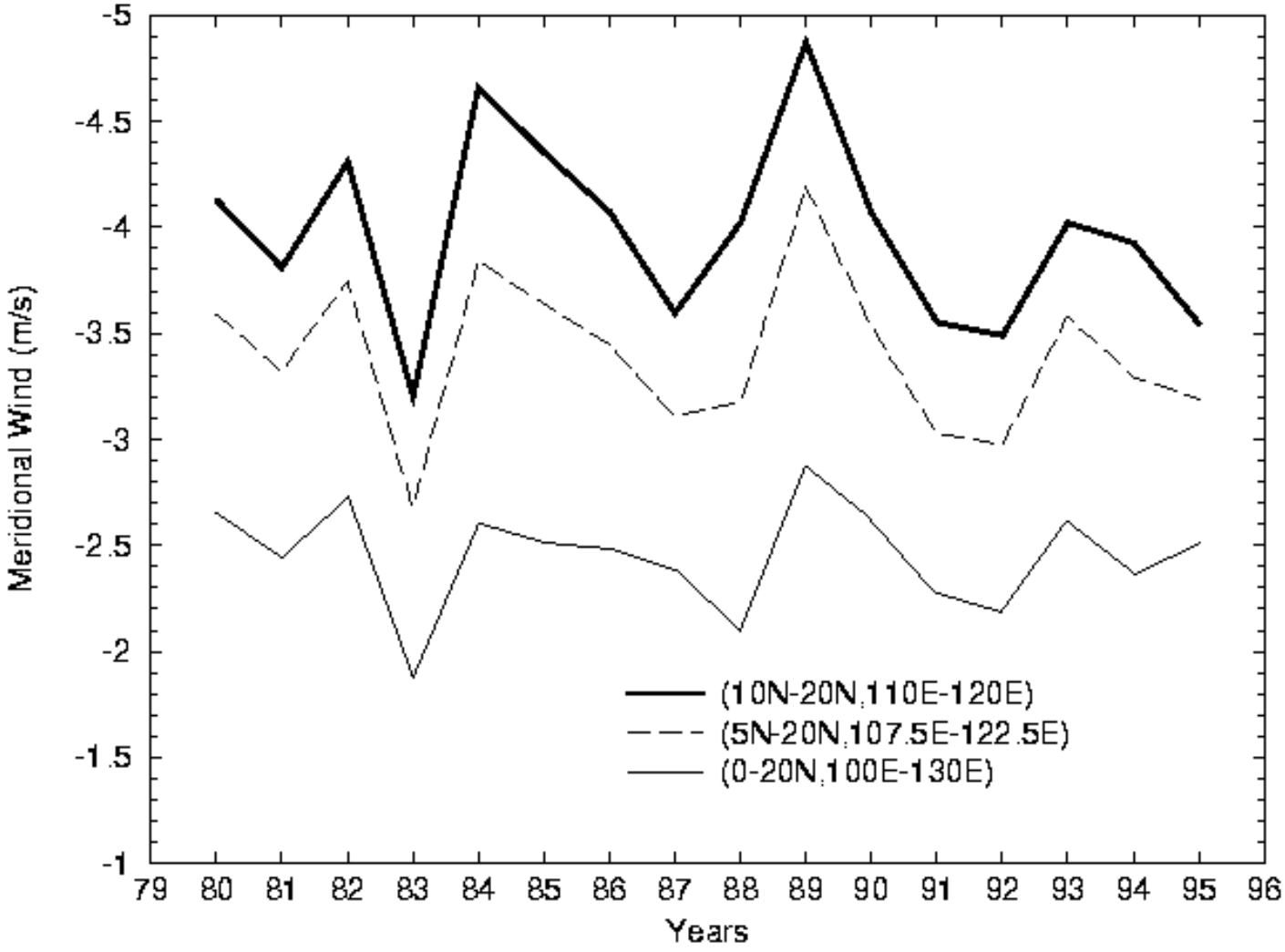

Fig. 13. Winter (NDJFM) area averaged northerly wind over the South China Sea (110°E-115°E; 10°N-20°N) at 925 hPa and 850 hPa. Unit: m s-1.

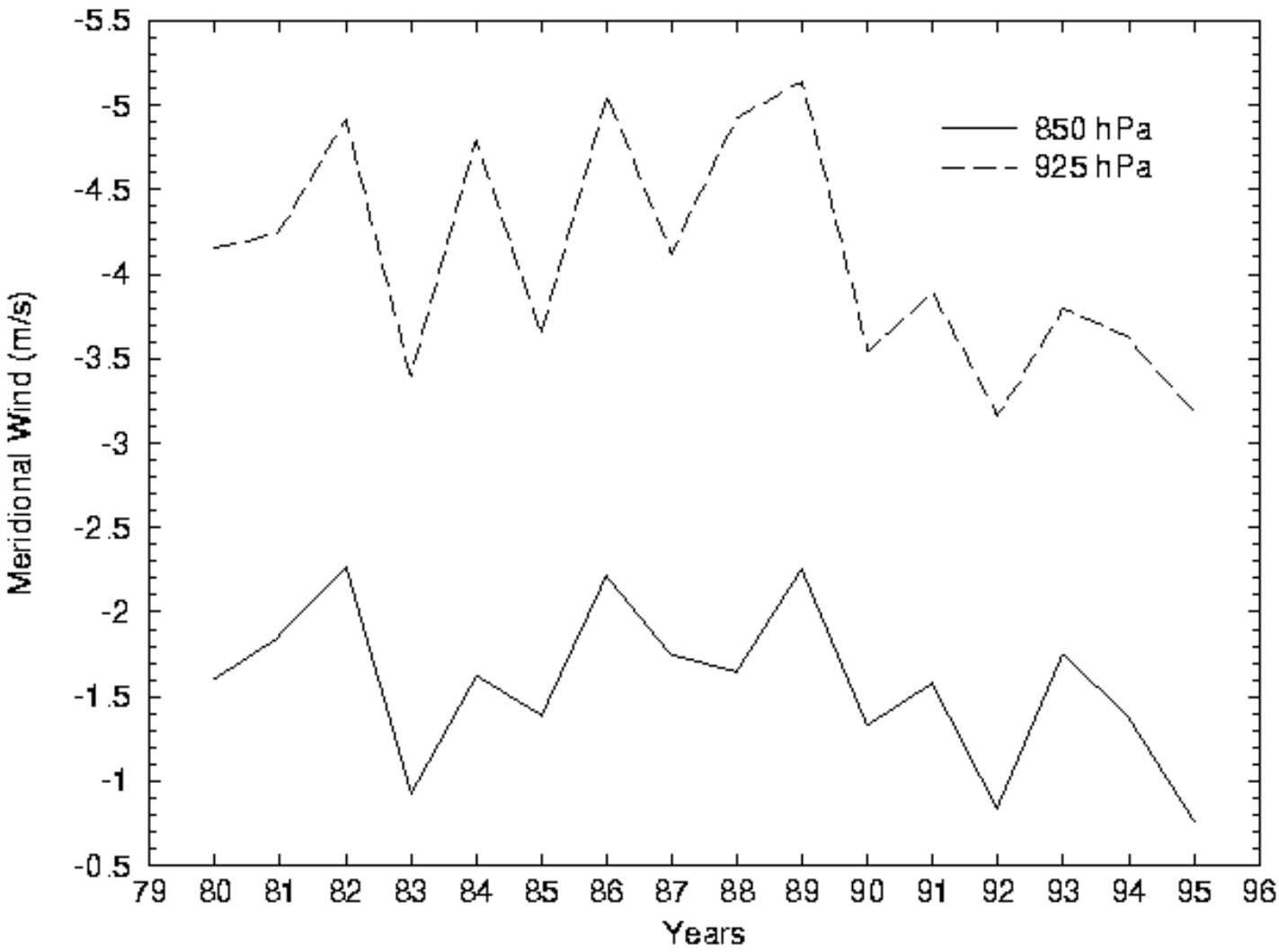

Fig. 14. Number of days that the Siberian high pressure exceeds 1050 hPa in the Siberia region (45°N-55°N, 90°E-110°E). Unit: number of days per season.

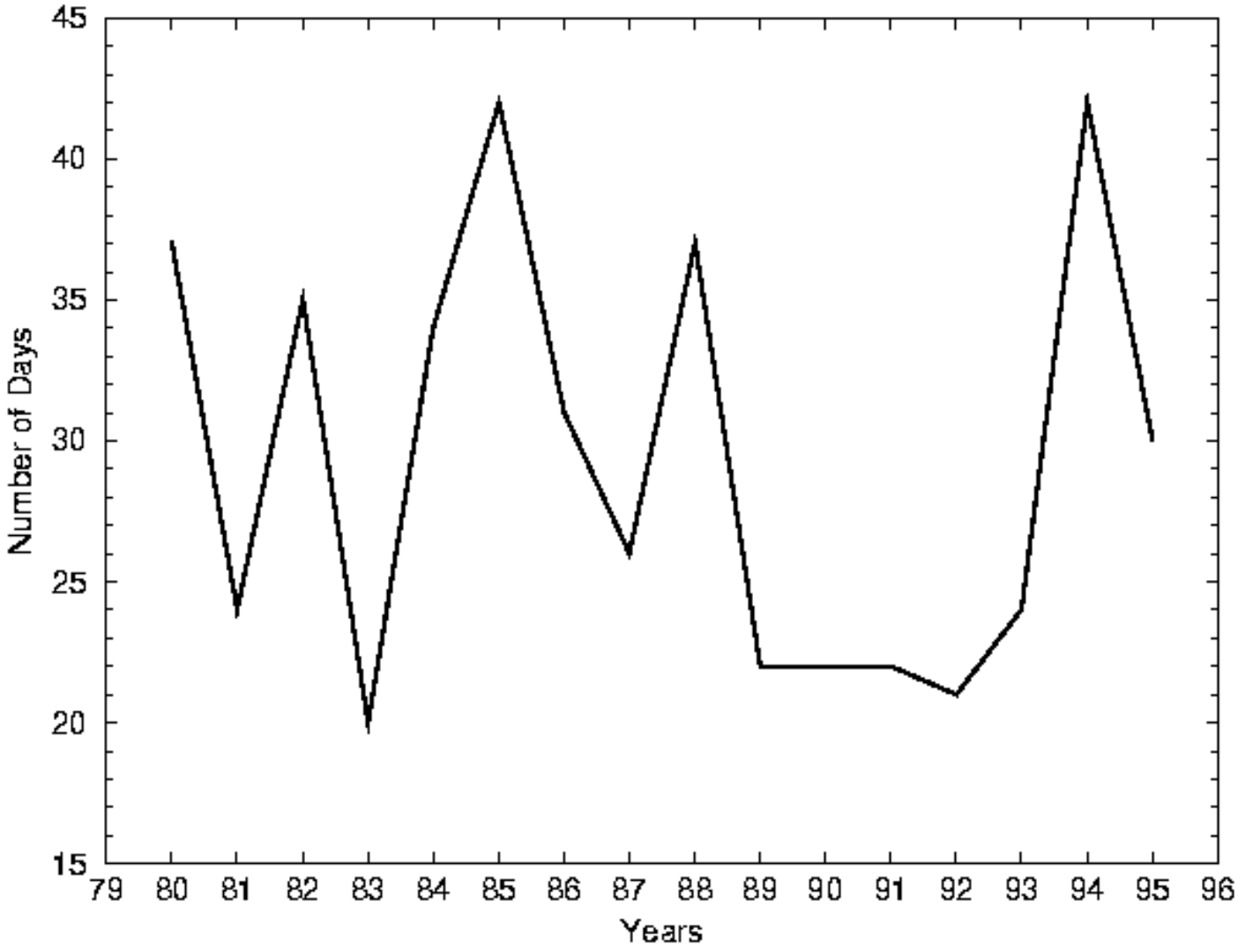

Fig. 6. Average lag correlations of region 3 surface air temperature with sea level pressure, surface air temperature, and surface v-wind (10m) for the period mid-November through mid-March for 1979/80-1994/95. Positive (negative) correlations ≥ 0.2 (≤ -0.2) are shaded white (black). For sea level pressure, negative correlations are plotted for R ≤ -0.2 at an interval of 0.1. For surface air temperature and v-wind, positive correlations are plotted for R 0.2 at an interval of 0.1. The use of $|R| \geq 0.2$ corresponds to the 95% confidence level for 100 degrees of freedom.

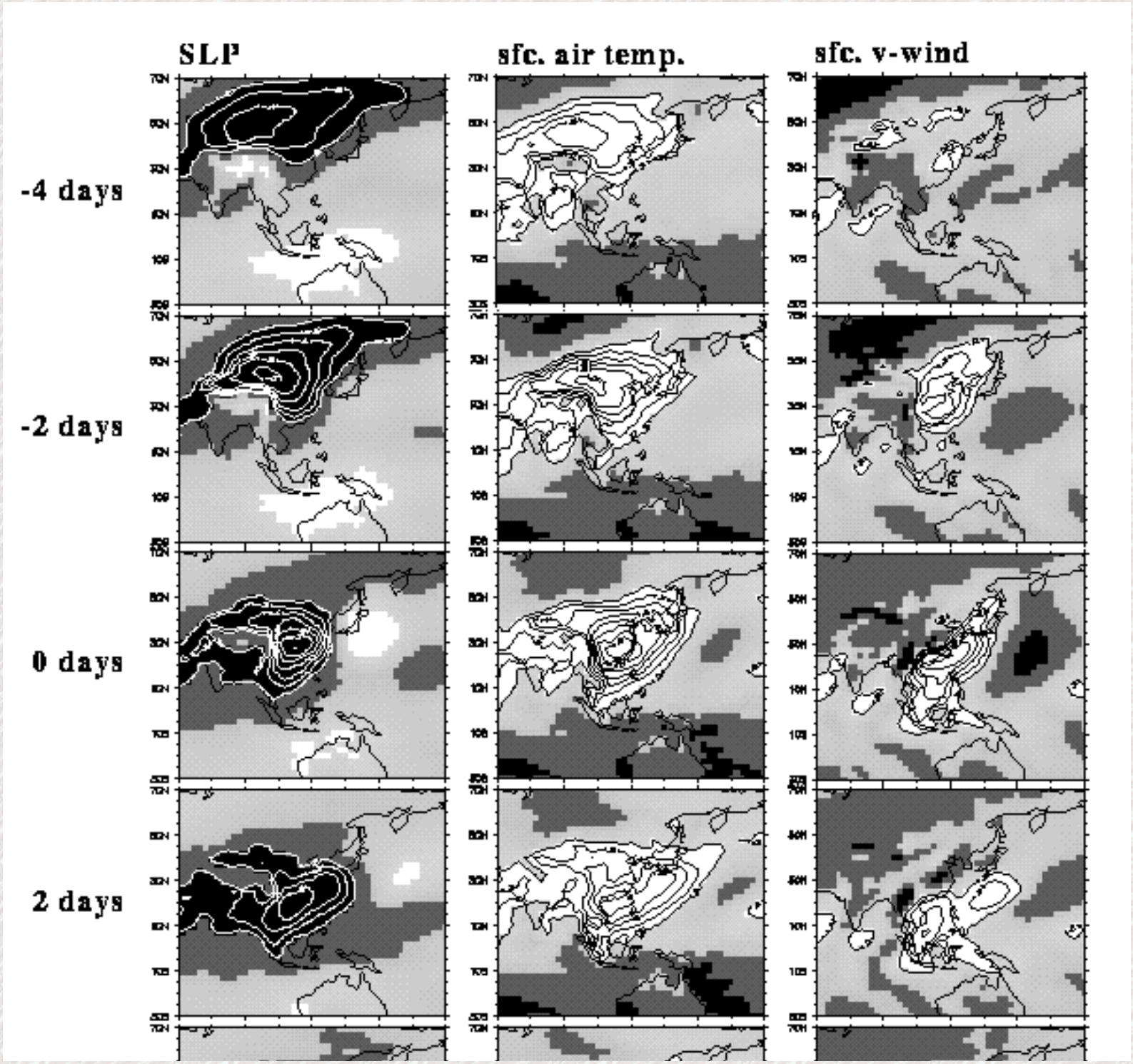

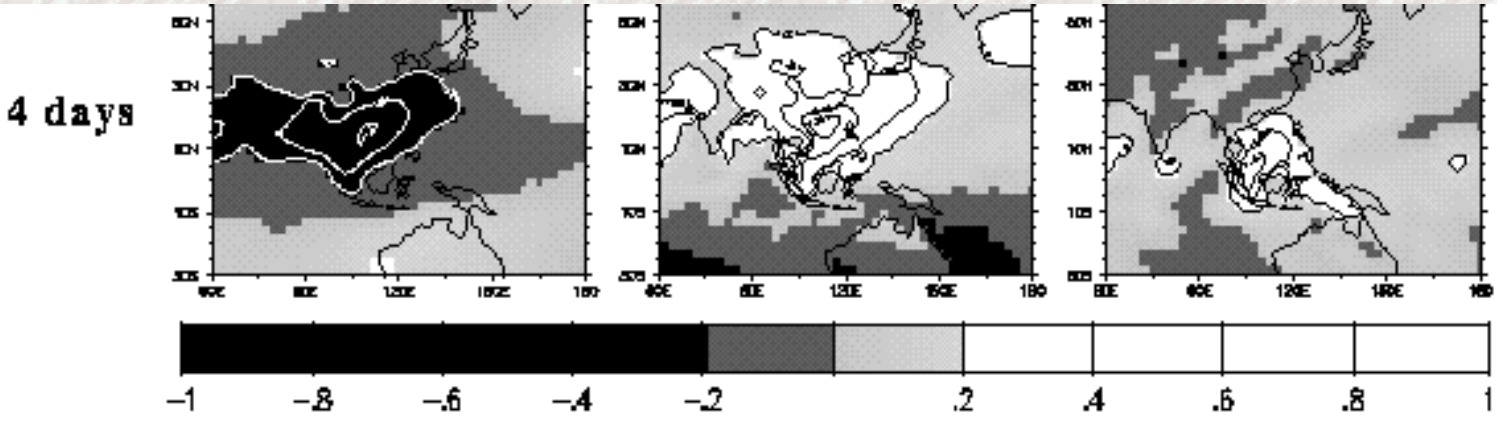
4 days
−1
−.8
−.6
−.4
−.2
.2
.4
.6
.8
1

Fig. 7. (a) Monthly distribution of number of cold surges. These variables are for the period of October - April of 1979/80-1994/95.

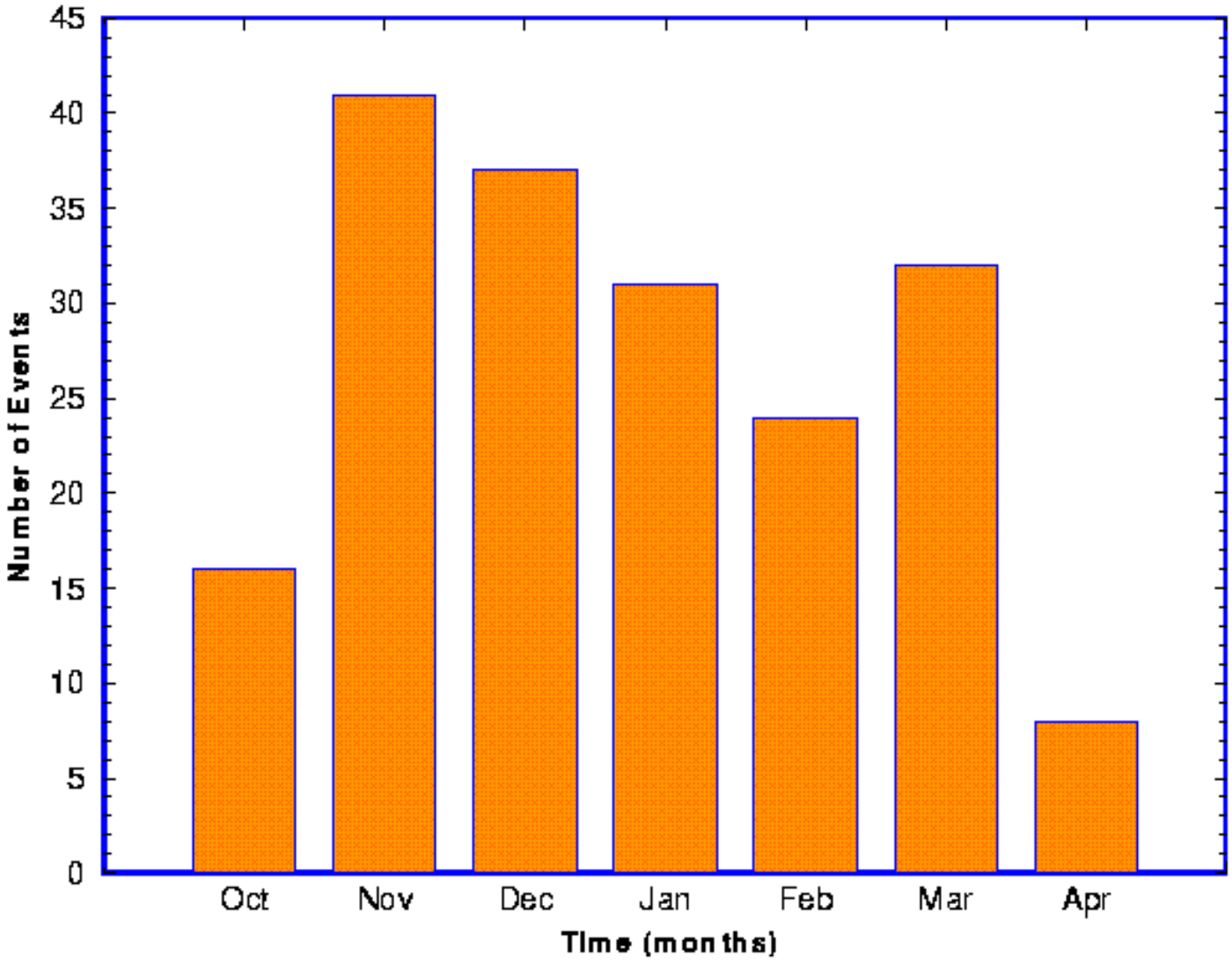

Fig. 7. (b) Monthly distribution of number of days that the Siberian high exceed 1050 hPa. These variables are for the period of October - April of 1979/80 - 1994/95.

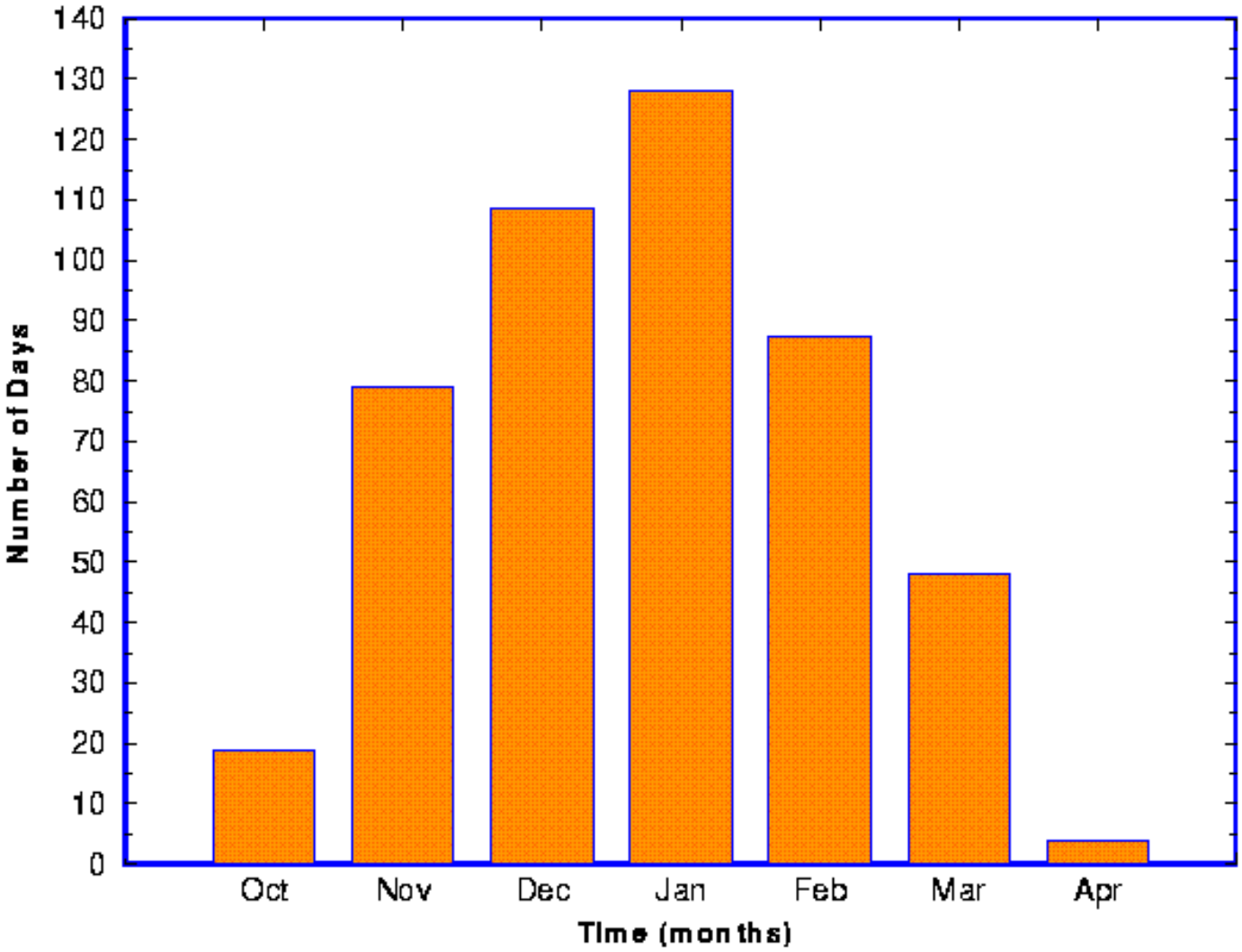

Fig. 8. Seasonal (NDJFM) averaged Southern Oscillation Index. Anomaly of pressure difference between Tahiti and Darwin. Unit: hPa. The year 1980 in the x-axis represents the winter of 1979/80 and so on. This applies to all the figures for interannual time series shown below.

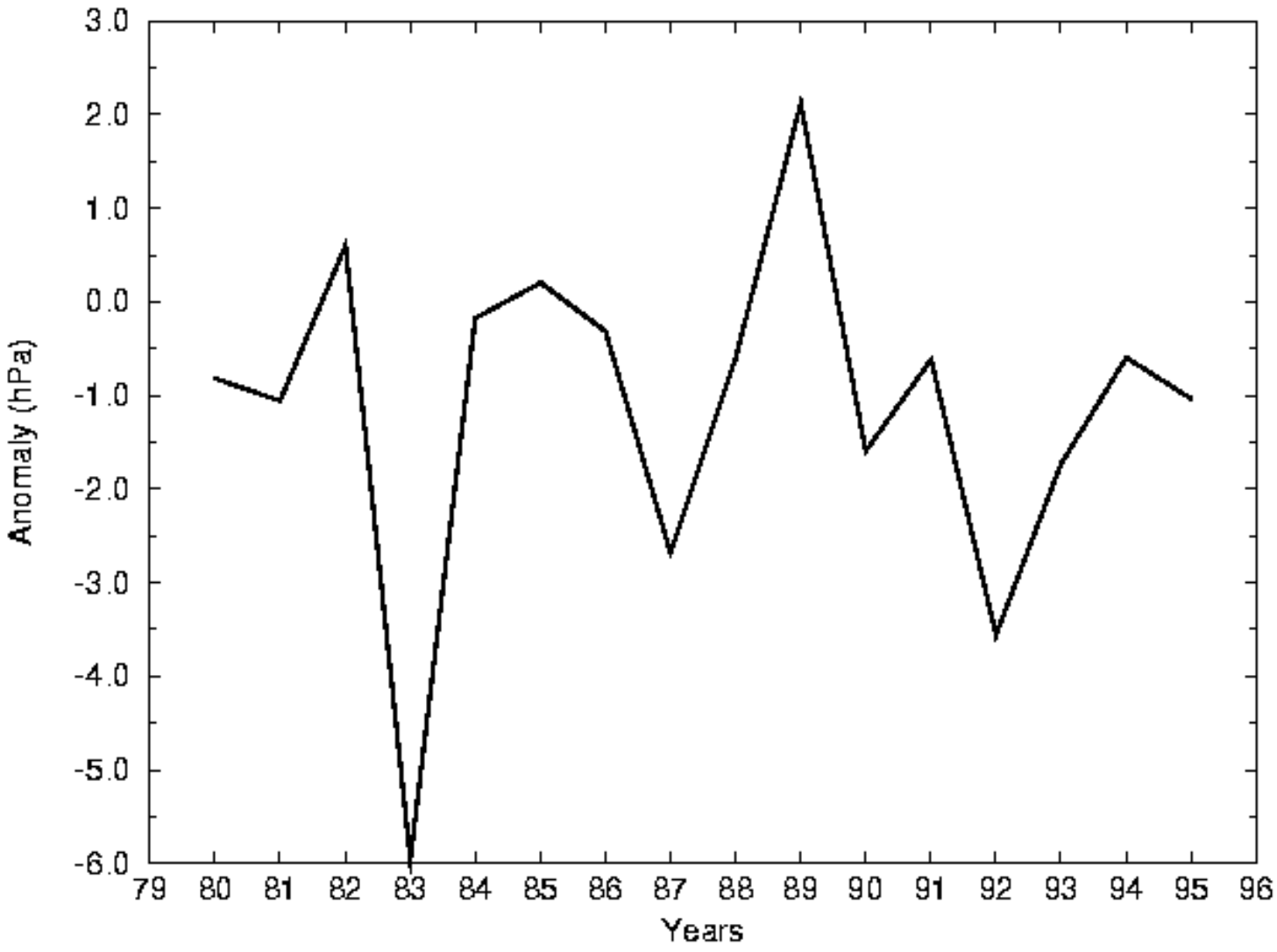

Fig. 9. Cold surge frequency from 1979/80-1994/95. Unit: number of events per season.

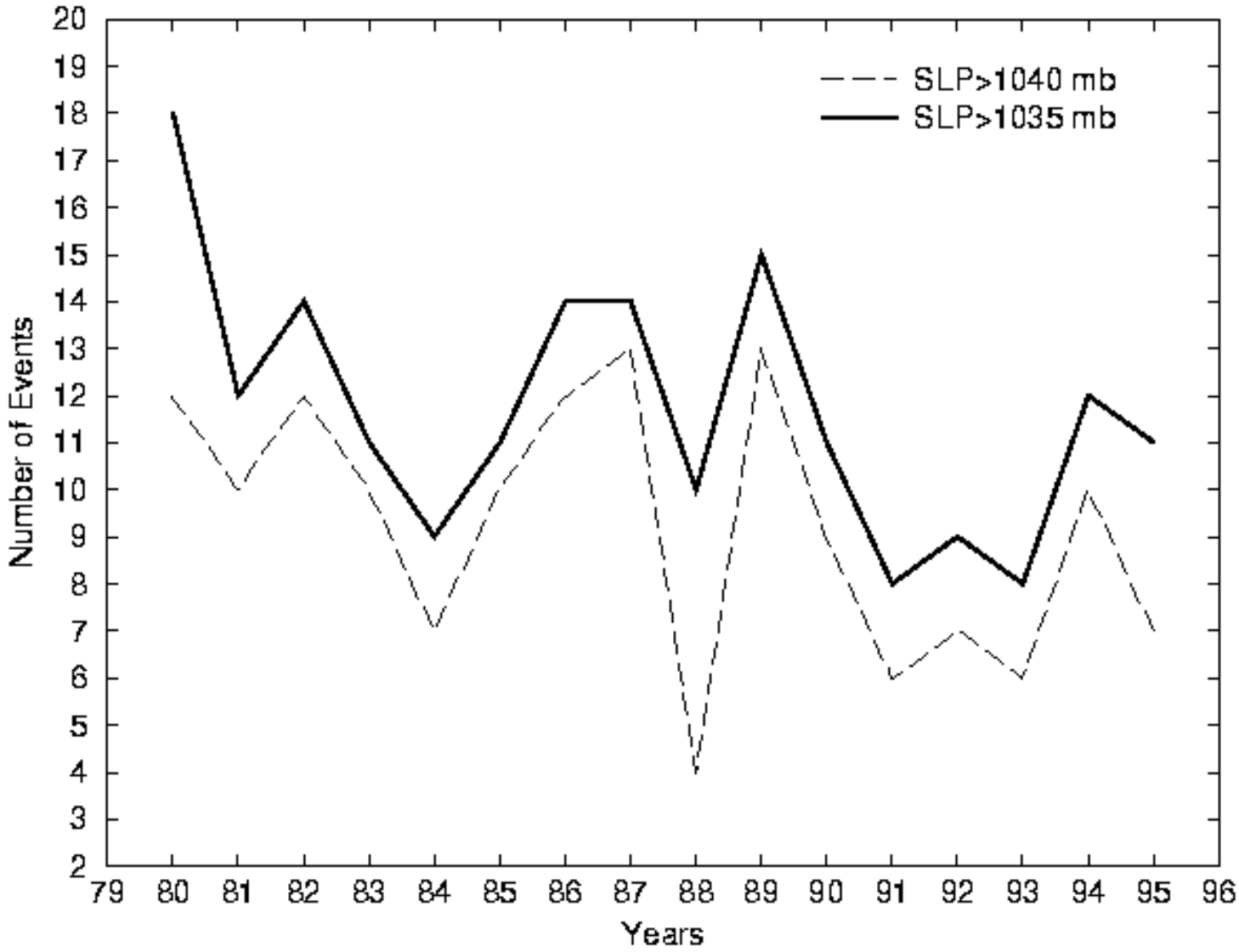

Fig. 10. (a) Twice daily time series of area averaged meridional wind from region 3, near Taiwan (120°E-125°E; 22.5°N-27.5°N), and in the vicinity of the South China Sea (110°E-115°E; 10°N-20°N). Unit: m/sec.

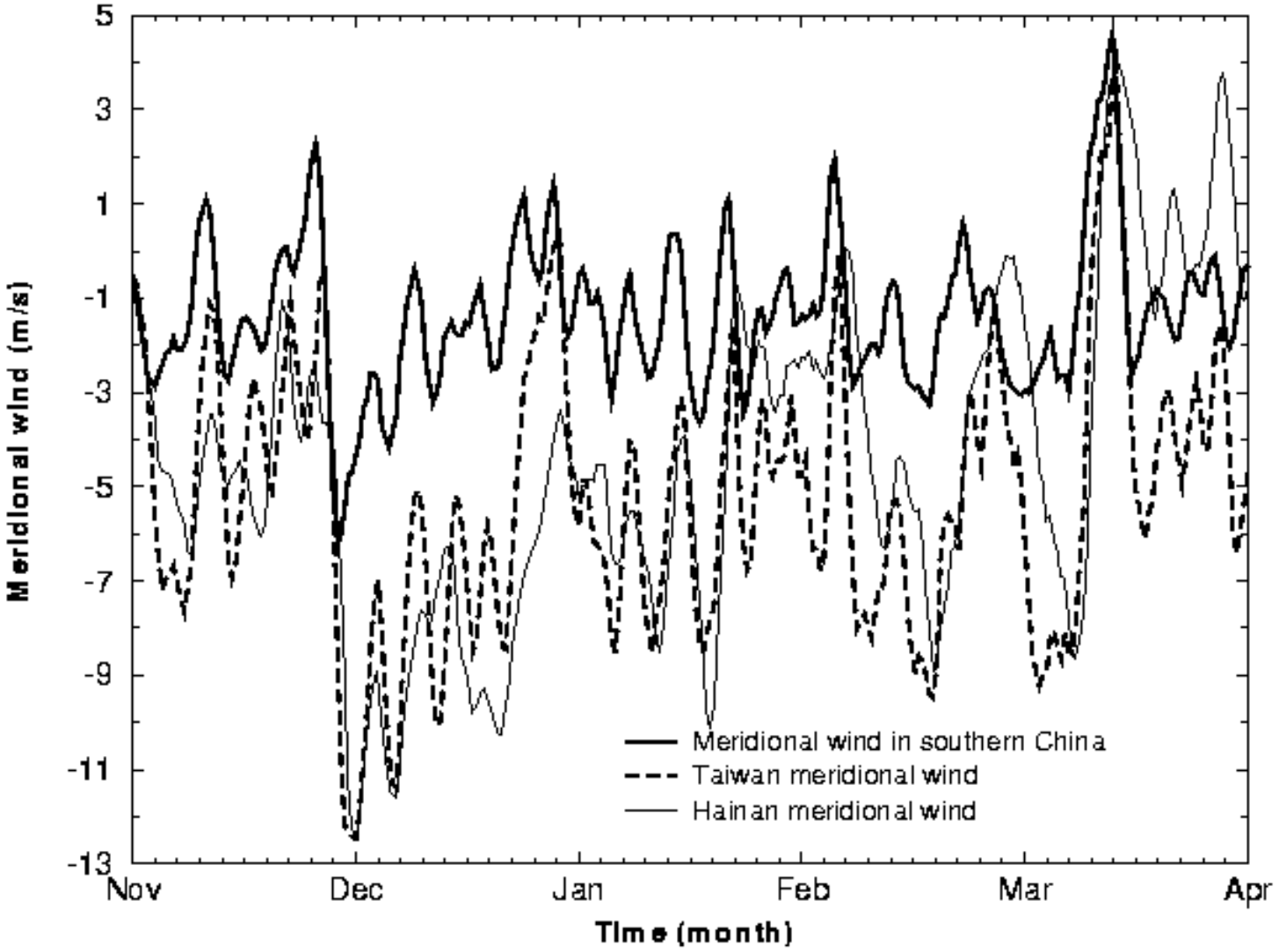

Figure 10. (b) Twice daily time series of region 1 SLP from November of 1987 to March of 1988. Unit: hPa. A five-point running average has been applied to all the fields.

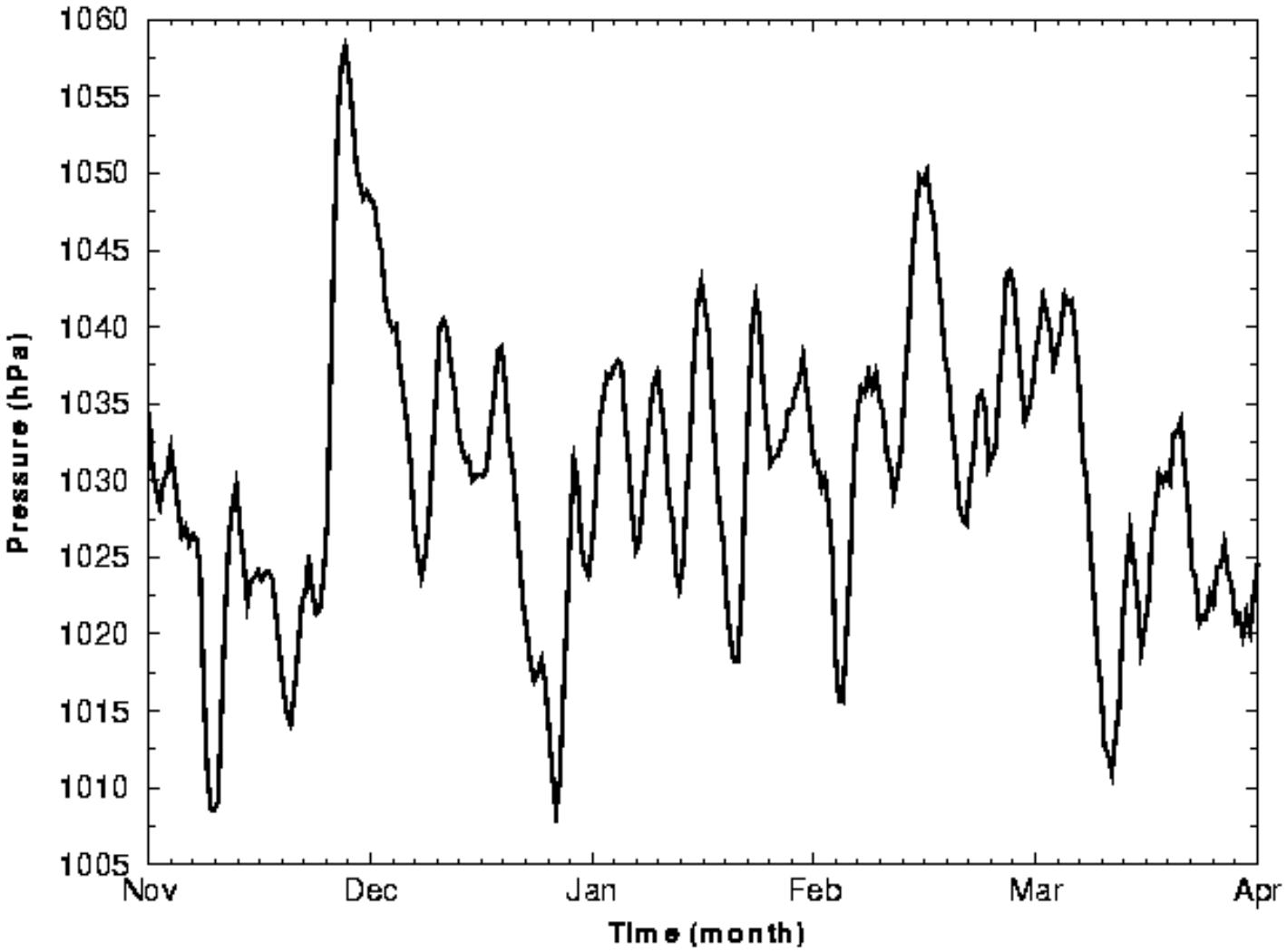

Fig. 11. Cold surge frequency in the South China Sea, number of days the maximum northerly wind near the South China Sea (110°E-120°E; 10°N-20°N) exceed 7 m/s. Unit: number of days per season.

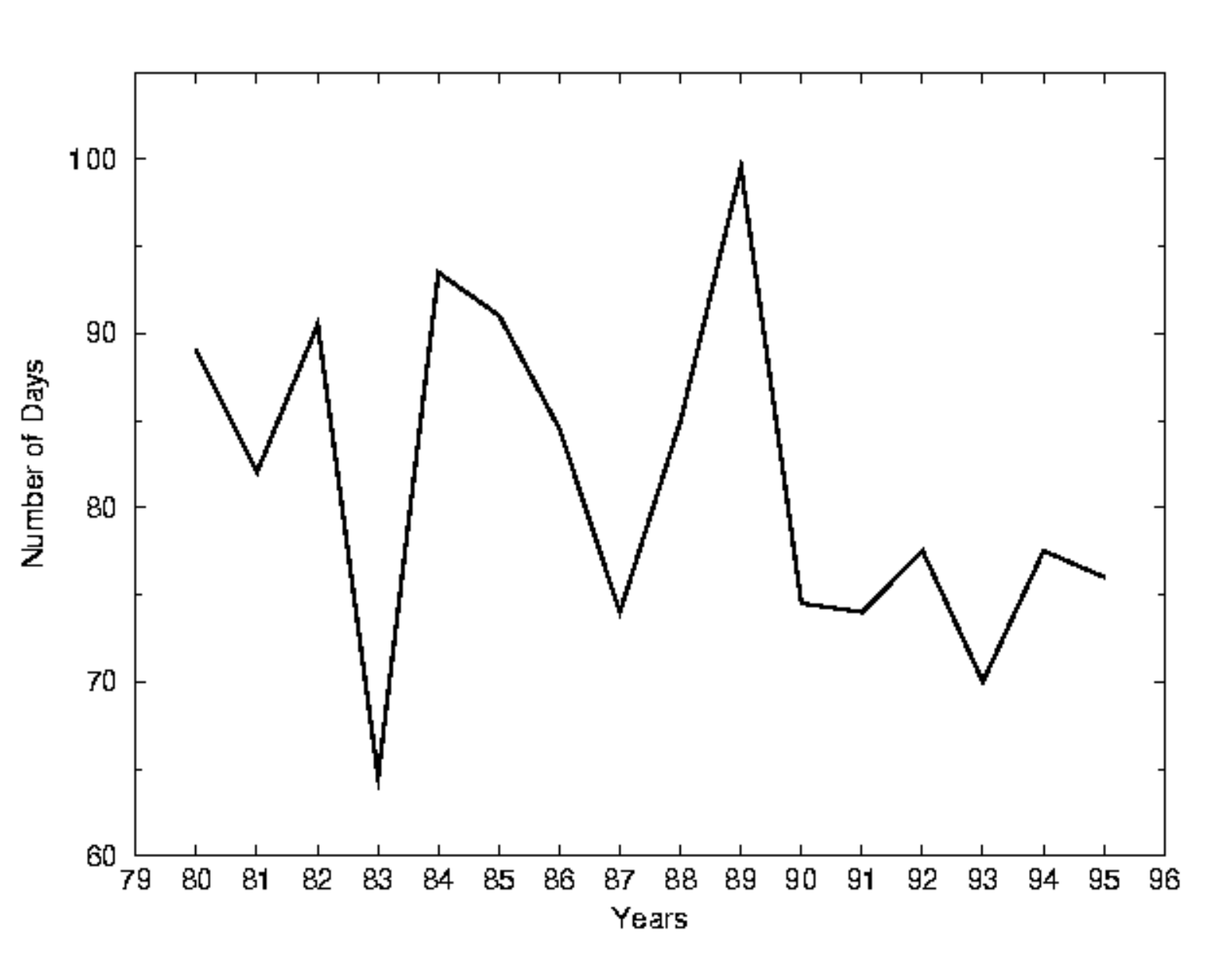

Fig. 12. Winter (NDJFM) area averaged northerly wind over three regions near the South China Sea and western Pacific. Unit: m s-1.

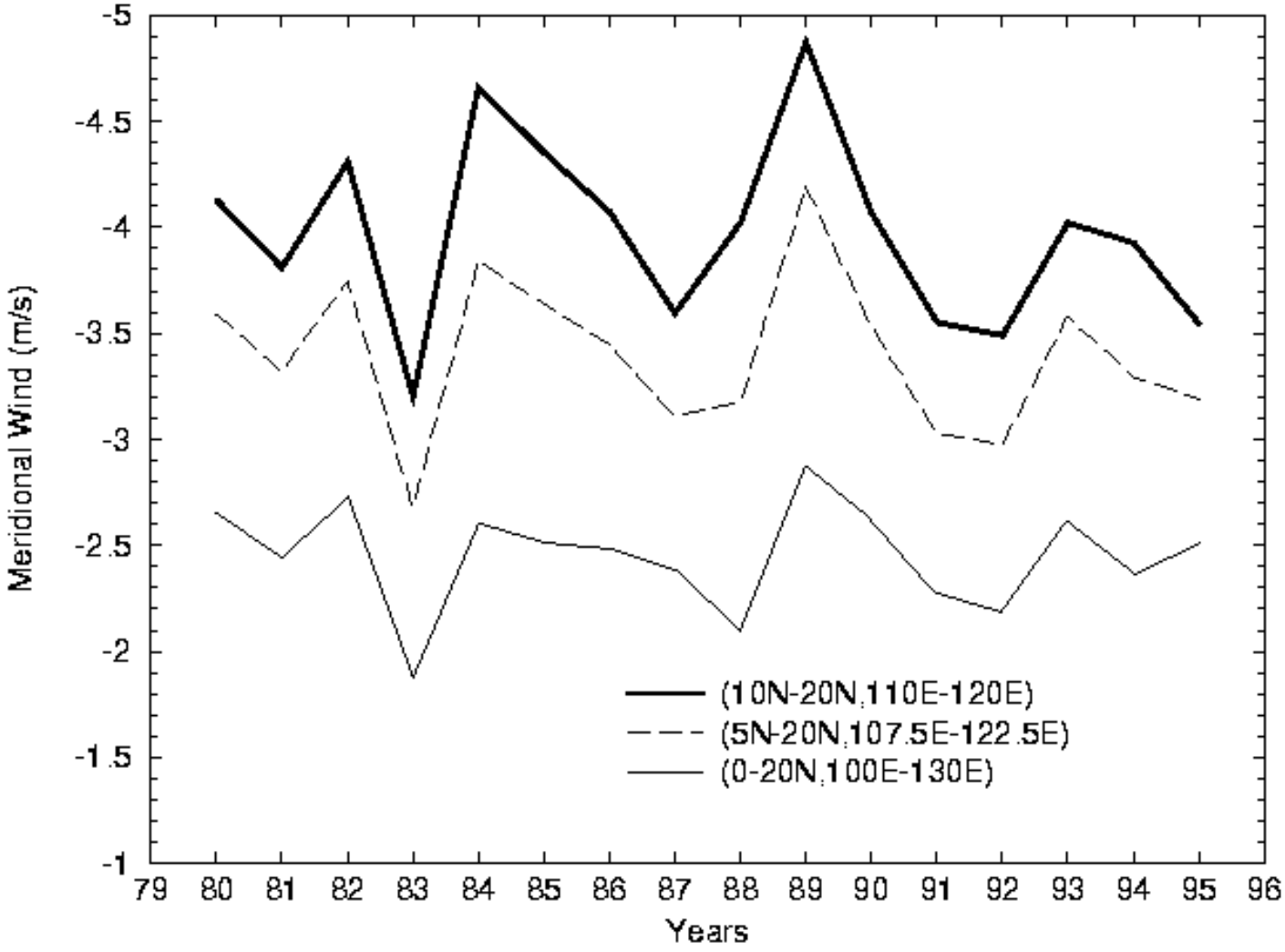

Fig. 13. Winter (NDJFM) area averaged northerly wind over the South China Sea (110°E-115°E; 10°N-20°N) at 925 hPa and 850 hPa. Unit: m s-1.

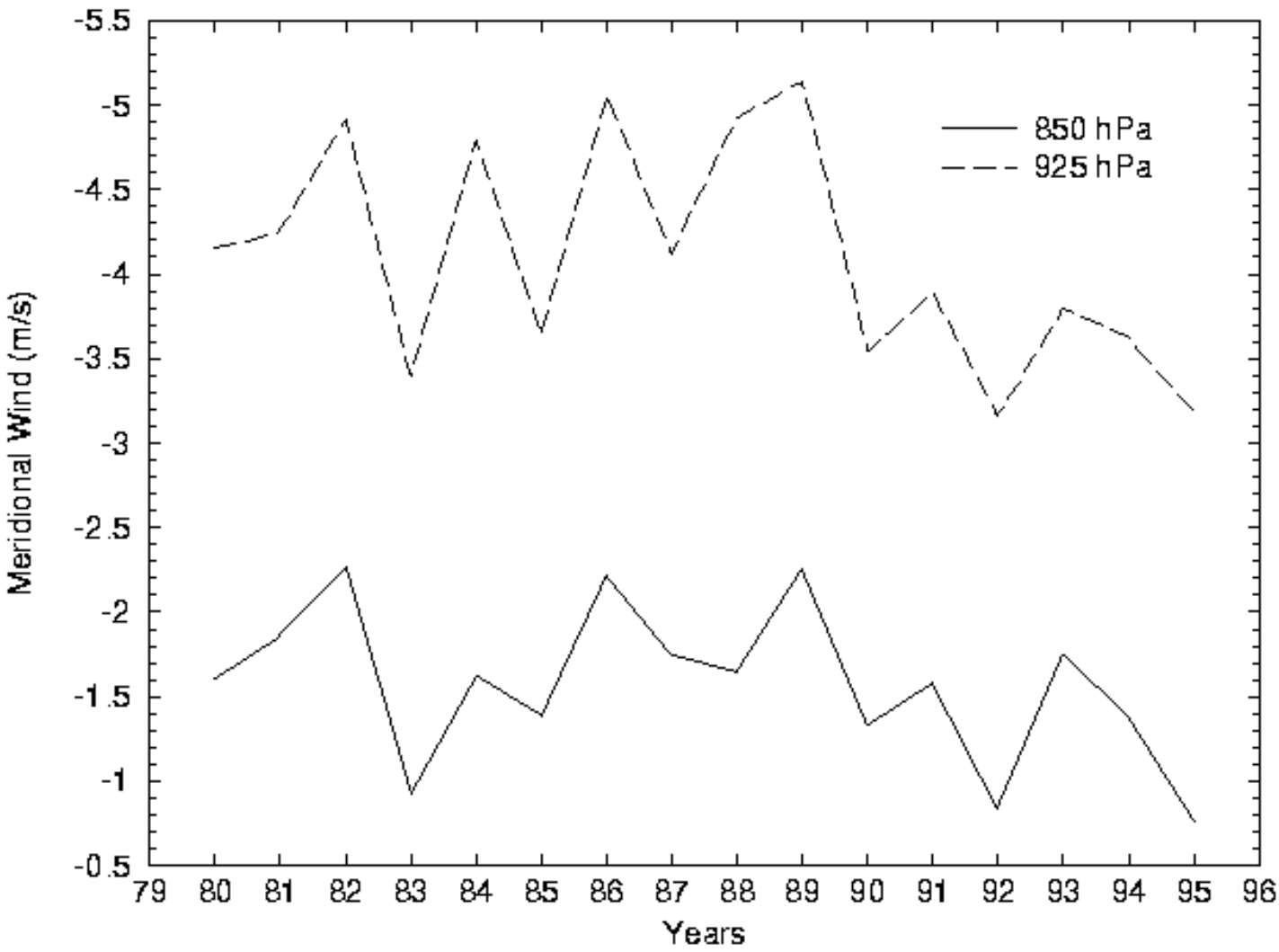

Fig. 14. Number of days that the Siberian high pressure exceeds 1050 hPa in the Siberia region (45°N-55°N, 90°E-110°E). Unit: number of days per season.